PHYSICAL REVIEW D **87,** 093011 (2013)

Octet to decuplet electromagnetic transition in a relativistic quark model

G. Ramalho[1] and K. Tsushima[2]

[1]*CFTP, Instituto Superior Técnico, Universidade Técnica de Lisboa, Avenida Rovisco Pais, 1049-001 Lisboa, Portugal*
[2]*CSSM, School of Chemistry and Physics, University of Adelaide, Adelaide, South Australia 5005, Australia*
(Received 28 February 2013; published 31 May 2013)

We study the octet to decuplet baryon electromagnetic transitions using the covariant spectator quark model and predict the transition magnetic dipole form factors for those involving the strange baryons. Utilizing $SU(3)$ symmetry, the valence quark contributions are supplemented by the pion cloud dressing based on the one estimated in the $\gamma^* N \to \Delta$ reaction. Although the valence quark contributions are dominant in general, the pion cloud effects turn out to be very important to describe the experimental data. We also show that other mesons besides the pion, in particular the kaon, may be relevant for some reactions such as $\gamma^* \Sigma^+ \to \Sigma^{*+}$, based on our analysis for the radiative decay widths of the strange decuplet baryons.

DOI: 10.1103/PhysRevD.87.093011 PACS numbers: 13.40.Gp, 12.39.Ki, 13.40.Hq, 14.20.Jn

I. INTRODUCTION

Low-lying baryons are classified into the spin $1/2$ octet and spin $3/2$ decuplet by quark models and quantum chromodynamincs (QCD). The electromagnetic structure of the octet (B) and decuplet (B') baryons, or the $\gamma^* B \to B'$ transition, can be characterized by their electromagnetic form factors. These form factors encode the microscopic quark and gluon QCD substructure of the baryons, but can also be represented in terms of the effective degrees of freedom, such as the baryon cores dressed by meson clouds.

Although there is abundant experimental information on the nucleon electromagnetic structure and the $\gamma^* N \to \Delta$ transition form factors [1–3], in particular, the studies of the other possible octet to decuplet electromagnetic transition form factors involving the strange baryons (baryons with one or more strange quarks) are nearly nonexistent. (The data can be found in Refs. [4–8].) In the past, several theoretical studies of the octet to decuplet electromagnetic transitions were performed in nonrelativistic and relativistic quark models [9–19], Skyrme and soliton models [20–22], QCD sum rules [23], chiral perturbation theory [24–26], large N_c limit [27], algebraic models of hadron structure [28], and lattice QCD [29]. In particular, lattice QCD studies for the $\gamma^* N \to \Delta$ reaction can be found in Refs. [30,31].

The study of the $\gamma^* B \to B'$ transition is very important to understand the role of the meson cloud. For the $\gamma^* N \to \Delta$ reaction, the meson cloud contributions are shown to be crucial [1,2,16,32,33]. Then, it is natural to investigate the role of the meson cloud also for the other octet to decuplet electromagnetic transitions. In order to understand the role of the meson cloud quantitatively, where the pion cloud is expected to be dominant, the prerequisite is to understand the valence quark contributions quantitatively.

For this purpose, we rely on the covariant spectator quark model [32–38], since it was successful in the studies of the electromagnetic structure of nucleon [39–41], octet and decuplet baryons [34–37,42–45], transition form factors of the reactions $\gamma^* N \to \Delta(1232)$, $\gamma^* N \to N^*(1440)$, $\gamma^* N \to N^*(1535)$ [32,33,46–48], and others [49,50]. We follow the formalism developed in Refs. [34,35] for the octet baryons and that in Ref. [37] for the decuplet baryons. In these works, the covariant spectator quark model was extended from the $SU(2)$ to the $SU(3)$ scheme for the lattice QCD regime and then extrapolated back to the physical regime. We also follow closely the study made for the $\gamma^* N \to \Delta$ transition based on an S-state approach to describe the nucleon and Δ systems [32], utilizing the $SU(3)$ meson-baryon coupling scheme. However, as is well known, the contributions solely from the valence quarks are insufficient to describe the observed cross sections and the extracted form factors for the $\gamma^* N \to \Delta$ reaction (especially the magnetic dipole form factor G_M^*). Therefore, explicit pion cloud effects for the other $\gamma^* B \to B'$ reactions involving the strange baryons should also be considered by extending the $\gamma^* N \to \Delta$ treatment based on an $SU(3)$ symmetry scheme, and this is done in the present study.

Since we adopt an S-state approximation for the octet and decuplet systems, the contributions for the electric and Coulomb quadrupole form factors will vanish, and only the contributions for the magnetic dipole form factor G_M^* will survive. Although this is an approximation, it is justified, since the electric and Coulomb form factors are known to be small compared to G_M^* in the $\gamma^* N \to \Delta$ reaction [1–3,33]. Then, in this article we will focus on the magnetic dipole form factor.

This article is organized as follows: In Sec. II we present the covariant spectator quark model, including the parametrizations for the octet and decuplet baryon wave functions and the quark electromagnetic current. Results of the form factors, both for the valence quark and pion cloud contributions, are presented in Sec. III. Section IV is devoted to

the final results and discussions. Summary and conclusions are given in Sec. V.

II. COVARIANT SPECTATOR QUARK MODEL

The covariant spectator quark model was derived from the covariant spectator theory [51]. In the model a baryon is described as a three-constituent quark system, where one quark is free to interact with the electromagnetic fields and a pair of noninteracting quarks is treated as a single on-mass-shell spectator particle (diquark) with an effective mass m_D [37,39,40]. The quark current is parametrized based on a vector meson dominance mechanism as explained in detail in Refs. [34,35,37,39].

The baryon wave function depends on the baryon momentum P, the diquark momentum k, the flavor indices, and the spin projections, as will be shown later. The wave function is constructed conveniently by the symmetrized states of the diquark pair (12), and the off-mass-shell quark 3. The transition current can be calculated in terms of the quark-3 states. To obtain the final, total contribution, we may multiply by a factor of 3 the current associated with the quark 3.

The covariant spectator quark model was also generalized to the lattice QCD regime with heavy pions, where the meson cloud effects are expected to be very small [37,46,47]. The fact that the same parametrization of the model holds for both the physical and the lattice QCD regimes gives us some confidence that the valence quark contributions calculated in the model are well under control.

Next, we will present the wave functions of the octet and decuplet baryons in the covariant spectator quark model. We will use M_B and $M_{B'}$ for the octet and decuplet baryon masses, respectively, and M_N for the nucleon mass.

A. Octet baryon wave functions

In general the octet baryon wave function (spin $1/2$) in an S state for the quark-diquark system can be written as [35,36]

$$\Psi_B(P,k) = \frac{1}{\sqrt{2}}\{\phi_S^0|M_A\rangle + \phi_S^1|M_S\rangle\}\psi_B(P,k), \tag{2.1}$$

where $|M_A\rangle$ and $|M_S\rangle$ are, respectively, the flavor antisymmetric and symmetric wave functions, ϕ_S^X ($X = 0, 1$) are the spin (0 and 1) wave functions, and ψ_B is the octet baryon B radial wave function to be defined shortly. Spin projection indices are suppressed for simplicity. The explicit expressions for the all-octet baryon members are presented in Table I. The spin wave functions are given by

$$\phi_S^0\left(+\frac{1}{2}\right) = \frac{1}{\sqrt{2}}(\uparrow\downarrow - \downarrow\uparrow)\uparrow, \tag{2.2}$$

$$\phi_S^1\left(+\frac{1}{2}\right) = -\frac{1}{\sqrt{6}}[(\uparrow\downarrow + \downarrow\uparrow)\uparrow - 2\uparrow\uparrow\downarrow], \tag{2.3}$$

and

$$\phi_S^0\left(-\frac{1}{2}\right) = \frac{1}{\sqrt{2}}(\uparrow\downarrow - \downarrow\uparrow)\downarrow, \tag{2.4}$$

$$\phi_S^1\left(-\frac{1}{2}\right) = \frac{1}{\sqrt{6}}[(\uparrow\downarrow + \downarrow\uparrow)\downarrow - 2\downarrow\downarrow\uparrow]. \tag{2.5}$$

This nonrelativistic structure is generalized to a relativistic form in the covariant spectator quark model [32,39],

$$\phi_S^0 = u(P), \qquad \phi_S^1 = -\varepsilon_\lambda^{\alpha*}(P)U^\alpha(P), \tag{2.6}$$

where

$$U^\alpha(P) = \frac{1}{\sqrt{3}}\gamma_5\left(\gamma^\alpha - \frac{P^\alpha}{M_B}\right)u(P). \tag{2.7}$$

In the above, $u(P)$ represents the Dirac spinor of the octet baryon B with momentum P and spin projection s, and $\varepsilon_\lambda(P)$ ($\lambda = 0, \pm 1$) the diquark polarization vector in the fixed-axis representation [39,41]. The spin projection is suppressed in the Dirac spinors and U^α for simplicity.

The radial wave function ψ_B is defined in terms of the dimensionless variable χ_B,

$$\chi_B = \frac{(M_B - m_D)^2 - (P-k)^2}{M_B m_D}, \tag{2.8}$$

where m_D is the diquark mass. Using the formalism of Refs. [34,35] we write ψ_B for $B = N, \Lambda, \Sigma, \Xi$,

TABLE I. Flavor wave functions of the octet baryons [35,36].

B	$\lvert M_S\rangle$	$\lvert M_A\rangle$
p	$\frac{1}{\sqrt{6}}[(ud+du)u - 2uud]$	$\frac{1}{\sqrt{2}}(ud-du)u$
n	$-\frac{1}{\sqrt{6}}[(ud+du)d - 2ddu]$	$\frac{1}{\sqrt{2}}(ud-du)d$
Λ^0	$\frac{1}{2}[(ds+sd)u - (us+su)d]$	$\frac{1}{\sqrt{12}}[(sd-ds)u - (su-us)d + 2(du-du)s]$
Σ^+	$\frac{1}{\sqrt{6}}[(us+su)u - 2uus]$	$\frac{1}{\sqrt{2}}(us-su)u$
Σ^0	$\frac{1}{\sqrt{12}}[(sd+ds)u + (su+us)d - 2(ud+du)s]$	$\frac{1}{2}[(ds-sd)u - (us-su)d]$
Σ^-	$\frac{1}{\sqrt{6}}[(sd+ds)d - 2dds]$	$\frac{1}{\sqrt{2}}(ds-sd)d$
Ξ^0	$-\frac{1}{\sqrt{6}}[(us+su)s - 2ssu]$	$\frac{1}{\sqrt{2}}(us-su)s$
Ξ^-	$-\frac{1}{\sqrt{6}}[(ds+sd)s - 2ssd]$	$\frac{1}{\sqrt{2}}(ds-sd)s$

$$\psi_N(P,k) = \frac{N_N}{m_D(\beta_1 + \chi_N)(\beta_2 + \chi_N)}, \quad (2.9)$$

$$\psi_\Lambda(P,k) = \frac{N_\Lambda}{m_D(\beta_1 + \chi_\Lambda)(\beta_3 + \chi_\Lambda)}, \quad (2.10)$$

$$\psi_\Sigma(P,k) = \frac{N_\Sigma}{m_D(\beta_1 + \chi_\Sigma)(\beta_3 + \chi_\Sigma)}, \quad (2.11)$$

$$\psi_\Xi(P,k) = \frac{N_\Xi}{m_D(\beta_1 + \chi_\Xi)(\beta_4 + \chi_\Xi)}, \quad (2.12)$$

where N_B are the normalization constants and β_i ($i = 1, 2, 3, 4$) are the momentum range parameters in units of m_D. We use the parameters determined in Ref. [34], namely, $\beta_1 = 0.0532$, $\beta_2 = 0.809$, $\beta_3 = 0.603$, and $\beta_4 = 0.381$, in which we obtain natural order for the size of the baryon cores [34].

The octet baryon masses can be described considering the pion-baryon $SU(3)$ couplings. We use the following experimental baryon mass values: $M_N = 0.939$ GeV, $M_\Lambda = 1.116$ GeV, $M_\Sigma = 1.192$ GeV, and $M_\Xi = 1.318$ GeV. The mass of the baryon B in the octet can be represented as $M_B = M_{0B} + \Sigma_0(M_B)$, where M_{0B} is a constant and $\Sigma_0(M_B)$ the self-energy at the pole position, which differs for the octet isomultiplet (N, Λ, Σ and Ξ) [36]. The self-energy is evaluated neglecting the diagrams with heavy mesons in the first approximation and can be expressed as $\Sigma_0 = G_{0B}\mathcal{B}_0$, where G_{0B} is a factor depending on the coupling of pion with the baryon B, and $\mathcal{B}_0$ is the value of the Feynman integral (with the coupling constants removed) with the mass M_B. The octet baryon masses can be reproduced with an accuracy better than 7% for the $SU(6)$ value $\alpha \equiv D/(F+D) = 0.6$ with $M_0 = 1.342$ GeV and $\mathcal{B}_0 = -0.127$ GeV [34]. The details of the $SU(3)$ couplings and coefficients G_{0B} are presented in Ref. [36].

B. Decuplet baryon wave functions

We write down the decuplet baryon wave functions in the S-state approximation for the quark-diquark system [37],

$$\Psi_{B'}(P,k) = -\psi_{B'}(P,k)\varepsilon^{\alpha *}_\lambda(P)u_\alpha(P)|B'\rangle, \quad (2.13)$$

where $|B'\rangle$ is the flavor state, u_α is the Rarita-Schwinger vector-spinor, and $\varepsilon_\lambda(P)$ is the diquark polarization vector in the decuplet baryon B' [41]. The explicit expressions are presented in Table II. The decuplet baryon radial wave functions $\psi_{B'}$, for $B' = \Delta, \Sigma^*, \Xi^*, \Omega$, are given by [37]

$$\psi_\Delta(P,k) = \frac{N_\Delta}{m_D(\alpha_1 + \chi_\Delta)^3}, \quad (2.14)$$

$$\psi_{\Sigma^*}(P,k) = \frac{N_{\Sigma^*}}{m_D(\alpha_1 + \chi_{\Sigma^*})^2(\alpha_2 + \chi_{\Sigma^*})}, \quad (2.15)$$

TABLE II. Quark flavor wave functions $|B'\rangle$ for the decuplet baryons [37].

B'	$\lvert B'\rangle$
Δ^{++}	uuu
Δ^{+}	$\frac{1}{\sqrt{3}}[uud + udu + duu]$
Δ^{0}	$\frac{1}{\sqrt{3}}[ddu + dud + udd]$
Δ^{-}	ddd
Σ^{*+}	$\frac{1}{\sqrt{3}}[uus + usu + suu]$
Σ^{*0}	$\frac{1}{\sqrt{6}}[uds + dus + usd + sud + dsu + sdu]$
Σ^{*-}	$\frac{1}{\sqrt{3}}[dds + dsd + sdd]$
Ξ^{*0}	$\frac{1}{\sqrt{3}}[uss + sus + ssu]$
Ξ^{*-}	$\frac{1}{\sqrt{3}}[dss + sds + ssd]$
Ω^{-}	sss

$$\psi_{\Xi^*}(P,k) = \frac{N_{\Xi^*}}{m_D(\alpha_1 + \chi_{\Xi^*})(\alpha_2 + \chi_{\Xi^*})^2}, \quad (2.16)$$

$$\psi_\Omega(P,k) = \frac{N_\Omega}{m_D(\alpha_2 + \chi_\Omega)^3}, \quad (2.17)$$

where $N_{B'}$ are the normalization constants and $\chi_{B'}$ is given by Eq. (2.8) with M_B replaced by $M_{B'}$. The wave function Ψ_Ω is also given for completeness. We use the parameters in Ref. [37], $\alpha_1 = 0.3366$ and $\alpha_2 = 0.1630$. A remark about the determination of these parameters is in order. The parameter α_1 was determined in Refs. [33,46], using a model with the dominant S-state contribution and very small D-state corrections, utilizing physical and lattice QCD data for the $\gamma^* N \to \Delta$ reaction. The same value of α_1 was used in Ref. [37]. In that work the lattice data for the decuplet electromagnetic form factors [52] were used to calibrate the value of α_2, neglecting the effects of the D states. This is justified by the smallness of the D-state contributions, observed previously in the $\gamma^* N \to \Delta$ transition (smaller than 1% in the Δ wave function) [46].

As for the decuplet baryon masses, they can also be described taking into account the self-energy corrections and the $SU(3)$ pion-baryon couplings. In this case we write $M_{B'} = M_{0B'} + \Sigma^*_0(M_{B'})$ with $\Sigma^*_0 = G_{1B'}\mathcal{B}_1 + G_{2B'}\mathcal{B}_2$, where the terms in $G_{1B'}$ and $G_{2B'}$ are, respectively, associated with the intermediate states of the octet and decuplet baryons and depend on the baryon flavors. $\mathcal{B}_1$ and $\mathcal{B}_2$ are the Feynman integrals, respectively, for an intermediate baryon of the octet and decuplet multiplet. See Appendix A for details. We can reproduce the decuplet masses, $M_\Delta = 1.232$ GeV, $M_{\Sigma^*} = 1.385$ GeV, $M_{\Xi^*} = 1.533$ GeV, and $M_\Omega = 1.672$ GeV, with a precision better than 0.1%, using $M_{0B'} = 1.672$ GeV, $\mathcal{B}_1 = -0.544$ GeV, and $\mathcal{B}_2 = -0.266$ GeV.

C. Transition current

The electromagnetic transition current J^μ, associated with the transition $\gamma^* B \to B'$, can be written in the relativistic impulse approximation [32,39,40],

$$J^\mu = 3\sum_\lambda \int_k \bar{\Psi}_{B'}(P_+, k) j_q^\mu(q) \Psi_B(P_-, k), \tag{2.18}$$

where P_+ (P_-) is the final (initial) baryon momentum, k the momentum of the on-shell diquark, and $j_q^\mu(q)$ is the quark current, depending on the transferred momentum $q = P_+ - P_-$ and on the quark flavor index (u, d or s). We represent the electromagnetic current in units of the proton charge e. Note the sum in the diquark polarization states ($\lambda = 0, \pm 1$). As mentioned already, the factor 3 takes into account the sum in the quarks based on the wave function symmetry. The integral symbol represents

$$\int_k = \int \frac{d^3\mathbf{k}}{2E_D(2\pi)^3}, \tag{2.19}$$

with $E_D = \sqrt{m_D^2 + \mathbf{k}^2}$.

D. Quark current

The quark current j_q^μ effectively parametrizes the constituent quark electromagnetic structure and thus includes the effects due to the gluon and meson dressing.

The operator j_q^μ has the generic structure [34,37,39,53],

$$j_q^\mu(q) = j_1\left(\gamma^\mu - \frac{\not{q} q^\mu}{q^2}\right) + j_2 \frac{i\sigma^{\mu\nu} q_\nu}{2M_N}, \tag{2.20}$$

where M_N is the nucleon mass and j_i ($i = 1, 2$) are flavor operators acting on the third quark in the $|M_A\rangle$ or $|M_S\rangle$ wave functions. For the quark current we use,

$$j_i = \frac{1}{6} f_{i+} \lambda_0 + \frac{1}{2} f_{i-} \lambda_3 + \frac{1}{6} f_{i0} \lambda_s, \quad (i = 1, 2), \tag{2.21}$$

where

$$\lambda_0 = \begin{pmatrix} 1 & 0 & 0 \\ 0 & 1 & 0 \\ 0 & 0 & 0 \end{pmatrix}, \qquad \lambda_3 = \begin{pmatrix} 1 & 0 & 0 \\ 0 & -1 & 0 \\ 0 & 0 & 0 \end{pmatrix}, \tag{2.22}$$

$$\lambda_s \equiv \begin{pmatrix} 0 & 0 & 0 \\ 0 & 0 & 0 \\ 0 & 0 & -2 \end{pmatrix} \tag{2.23}$$

are the flavor matrices. These operators act on the quark wave function in flavor space $q^T = (uds)$. The functions $f_{i\pm}(Q^2)$ with $Q^2 = -q^2$ are the quark form factors (see Ref. [34] for details) and are normalized as $f_{1\pm}(0) = 1$, $f_{2+}(0) = \kappa_+$, $f_{2+}(0) = \kappa_-$, and $f_{20}(0) = \kappa_0$. We can represent the isoscalar (κ_+), isovector (κ_-), and κ_0 in terms of the quark $q = u$, d, s anomalous magnetic moments, defining κ_q by $e_q \kappa_q \equiv j_2(0)$, where e_q is the quark charge. One obtains then $\kappa_+ = 2\kappa_u - \kappa_d$, $\kappa_- = \frac{1}{3}(2\kappa_u + \kappa_d)$, and $\kappa_0 = \kappa_s$. The values of the quark anomalous magnetic moments were fixed in the previous works as $\kappa_u = 1.711$, $\kappa_d = 1.987$, and $\kappa_s = 1.462$ [34,37].

Note that the values for the quark anomalous magnetic moments κ_q, defined according to Eq. (2.20), are expressed in units of nuclear magneton. In a naive conversion one can use the constituent quark mass $m_q \approx M_N/3$, which gives a factor of $1/3$. In the covariant spectator quark model, the anomalous magnetic moment takes into account the internal structure of the constituent quark. A simple estimate of the lowest-order effect of the gluon to the electromagnetic vertex gives $\kappa_q \simeq 1.5$ [39]. Therefore, deviations from the value 1.5 can be interpreted as a consequence of the internal electromagnetic structure. To compare our results with those of the quark anomalous magnetic moment usually found in the literature, κ_q', where the quark charge e_q is included in the definition, we use $\kappa_q' = \frac{1}{3} e_q \kappa_q$. We obtain then $\kappa_u' = 0.380$, $\kappa_d' = -0.221$, and $\kappa_s' = -0.162$ [assuming $m_s = m_u, m_d$, according to $SU(3)$].

Our values for κ_u' and κ_d' are close to the results of others such as the naive quark model [54], and calculations based on Dyson-Schwinger formalism [55,56], but are larger in absolute values than the other models such as, for instance, light-front constituent quark models [57] and the direct estimates of meson-cloud corrections [58] ($\kappa_u' \simeq 0.1$; $\kappa_d' = -0.15, -0.1$).

The inclusion of the term $-\not{q} q^\mu/q^2$ in the quark current (2.20) is equivalent to using the Landau prescription [59,60] to the final electromagnetic current (2.18). The term restores current conservation but does not affect the results of the observables [59]. In the present study the correction term gives no contribution to the transition current (2.18), since the octet and decuplet states are orthogonal.

III. ELECTROMAGNETIC FORM FACTORS

The $\gamma^* B \to B'$ transition current, for the case of the initial B spinor u with momentum P_- and the final B' vector-spinor u_β with momentum P_+, can be expressed as [32]

$$J^\mu = \bar{u}_\beta(P_+)[G_1 q^\beta \gamma^\mu + G_2 q^\beta P^\mu + G_3 q^\beta q^\mu - G_4 g^{\beta\mu}]\gamma_5 u(P_-), \tag{3.1}$$

where $P = \frac{1}{2}(P_+ + P_-)$. For simplicity the B and B' spin projections are suppressed. In the above, G_i ($i = 1, 2, 3, 4$) are the octet to decuplet baryon transition form factors. Only three of them are independent. The current conservation leads to the condition [32]

$$G_4 = (M_{B'} + M_B) G_1 + \frac{1}{2}(M_{B'}^2 - M_B^2) G_2 - Q^2 G_3. \tag{3.2}$$

One can convert the form factors G_i ($i = 1, 2, 3$) into the multipole form factors defined by Jones and Scadron [61],

$$G_M^* = K\Big\{[(3M_{B'} + M_B)(M_{B'} + M_B) + Q^2]\frac{G_1}{M_{B'}} + (M_{B'}^2 - M_B^2) G_2 - 2Q^2 G_3\Big\}, \tag{3.3}$$

$$G_E^* = K\Big\{(M_{B'}^2 - M_B^2 - Q^2)\frac{G_1}{M_{B'}} + (M_{B'}^2 - M_B^2)G_2 - 2Q^2 G_3\Big\}, \tag{3.4}$$

$$G_C^* = K\{4M_{B'}G_1 + (3M_{B'}^2 + M_B + Q^2)G_2 + 2(M_{B'}^2 - M_B^2 - Q^2)G_3\}, \tag{3.5}$$

with

$$K = \frac{M_B}{3(M_{B'} + M_B)}. \tag{3.6}$$

Hereafter, we use G_X^* with $X = M, E, C$ to represent, respectively, the magnetic dipole, electric quadrupole, and Coulomb quadrupole form factors.

Next, we consider a decomposition, $G_X^* = G_X^b + G_X^\pi$, where G_X^b is the contribution from the quark core (valence quark contribution) and G_X^π the pion cloud contribution.

A. Valence quark contributions

Inserting the octet baryon B and decuplet baryon B' wave functions, respectively, given by Eqs. (2.1) and (2.13) into the transition current (2.18), we calculate the valence quark contributions for the current and form factors.

To perform the sum in the flavors associated with the octet and decuplet baryons, we follow the procedure given in Refs. [36,37] with $|B\rangle$ and $|B'\rangle$ shown in Tables I and II, and define

$$j_i^A \equiv 3\langle B'|j_i|M_A\rangle, \qquad (i = 1, 2), \tag{3.7}$$

$$j_i^S \equiv 3\langle B'|j_i|M_S\rangle, \qquad (i = 1, 2). \tag{3.8}$$

The explicit results for j_i^S are presented in Table III. As for j_i^A, one has $j_i^A \equiv 0$, which reflects the orthogonality between the spin-0 component of the octet baryon and the spin-1 component of the decuplet baryon wave functions, since the spin 3/2 states can have only spin-1 diquarks.

Once the coefficients j_i^S are determined, we can calculate a factor f_v and use the result of the current for the S-state approximation given by Ref. [32]. One can write

TABLE III. Coefficients j_i^S $(i = 1, 2)$ necessary to calculate the valence quark contributions for the form factors.

	j_i^S
$\gamma^* p \to \Delta^+$	$\sqrt{2}f_{i-}$
$\gamma^* n \to \Delta^0$	$\sqrt{2}f_{i-}$
$\gamma^*\Lambda \to \Sigma^{*0}$	$\sqrt{\frac{3}{2}}f_{i-}$
$\gamma^*\Sigma^+ \to \Sigma^{*+}$	$\frac{\sqrt{2}}{6}(f_{i+} + 3f_{i-} + 2f_{i0})$
$\gamma^*\Sigma^0 \to \Sigma^{*0}$	$\frac{\sqrt{2}}{6}(f_{i+} + 2f_{i0})$
$\gamma^*\Sigma^- \to \Sigma^{*-}$	$\frac{\sqrt{2}}{6}(f_{i+} - 3f_{i-} + 2f_{i0})$
$\gamma^*\Xi^0 \to \Xi^{*0}$	$\frac{\sqrt{2}}{6}(f_{i+} + 3f_{i-} + 2f_{i0})$
$\gamma^*\Xi^- \to \Xi^{*-}$	$\frac{\sqrt{2}}{6}(f_{i+} - 3f_{i-} + 2f_{i0})$

$$J^\mu = \frac{1}{\sqrt{3}}f_v \mathcal{I} \times \bar{u}_\beta(P_+)[2AM_{B'}q^\beta\gamma^\mu - 2Aq^\beta P^\mu - Aq^\beta q^\mu - g^{\beta\mu}]\gamma_5 u(P_-), \tag{3.9}$$

with $A = \frac{2}{(M_{B'}+M_B)^2+Q^2}$ and

$$\mathcal{I}(Q^2) = \int_k \psi_{B'}(P_+, k)\psi_B(P_-, k), \tag{3.10}$$

$$f_v(Q^2) = \frac{1}{\sqrt{2}}\Big\{j_1^S(Q^2) + \frac{M_{B'} + M_B}{2M_N}j_2^S(Q^2)\Big\}, \tag{3.11}$$

where Eqs. (3.10) and (3.11) are, respectively, the overlap of the radial wave functions and the symmetric flavor coefficient (corresponding to the isovector coefficient in the $\gamma^* N \to \Delta$ reaction).

From the relations above, one can derive

$$G_1 = AM_{B'}G_4, \tag{3.12}$$

$$G_2 = -AG_4, \tag{3.13}$$

$$G_3 = -\frac{1}{2}AG_4, \tag{3.14}$$

with

$$G_4 = \frac{2}{\sqrt{3}}f_v\mathcal{I}. \tag{3.15}$$

The valence quark contributions are then given by

$$G_M^b = \frac{8}{3\sqrt{3}}\frac{M_B}{M_{B'} + M_B}f_v\mathcal{I}, \tag{3.16}$$

$$G_E^b \equiv 0, \tag{3.17}$$

$$G_C^b \equiv 0. \tag{3.18}$$

The result for G_M^b depends on the details of the baryon structure, namely the radial wave functions ψ_B and $\psi_{B'}$, through the integral $\mathcal{I}$. For $Q^2 = 0$ one can prove that $\mathcal{I}(0) \le 1$, establishing the upper limit of $G_M^b(0)$ as $\overline{G_M^b}(0) = \frac{8}{3\sqrt{3}}\frac{M_B}{M_{B'}+M_B}f_v(0)$. The results are given in Table IV. Note, however, that $\overline{G_M^b}(0)$ provides only an upper limit. As shown in Appendix B, when $M_B < M_{B'}$ one has always $\mathcal{I}(0) < 1$, therefore $G_M^b(0) < \overline{G_M^b}(0)$.

The expressions (3.16), (3.17), and (3.18) show, as mentioned already, that when we use the S-state approximation for the octet and decuplet wave functions, one has only nonvanishing contributions for the magnetic dipole form factor G_M^*.

In Table IV we also compare our results for $\overline{G_M^b}(0)$ with an estimate of a valence quark model (QM) [11,29] and the results from quenched lattice QCD [29] (small meson cloud effects). Our purpose is to show that the valence quark contribution for $G_M^*(0)$ is bounded and insufficient to

TABLE IV. Upper limit of the magnetic dipole transition form factors for $Q^2 = 0$, $\overline{G_M^b}(0)$, which are independent of the baryon wave function parametrizations, compared with the results of quark models [11,29] and lattice QCD with $m_\pi = 662$ MeV [29].

	$\overline{G_M^b}(0)$	QM	Lattice
$\gamma^* p \to \Delta^+$	2.05	1.88	1.97(12)
$\gamma^* n \to \Delta^0$	2.05	1.88	1.97(12)
$\gamma^* \Lambda \to \Sigma^{*0}$	2.02		
$\gamma^* \Sigma^+ \to \Sigma^{*+}$	2.30	2.34	2.03(14)
$\gamma^* \Sigma^0 \to \Sigma^{*0}$	1.07	0.99	0.92(5)
$\gamma^* \Sigma^- \to \Sigma^{*-}$	−0.17	−0.36	−0.20(4)
$\gamma^* \Xi^0 \to \Xi^{*0}$	2.47	2.72	2.10(8)
$\gamma^* \Xi^- \to \Xi^{*-}$	−0.19	−0.42	−0.202(28)

explain the experimental results. Taking the $\gamma^* N \to \Delta$ case as an example, our estimate, the QM result, and the lattice QCD results give $G_M^*(0) \approx 2$, while the experimental result is 3.02 ± 0.03 [4]. Therefore, the valence quark contribution explains only about 70% of the experimental result.

For the $\gamma^* N \to \Delta$ reaction, one has also the results of the quenched lattice simulation from Alexandrou *et al.* [31], where the extrapolated quenched results gave $G_M^*(0) \simeq 2.1$ for $m_\pi = 563$ MeV; $G_M^*(0) \simeq 1.9$ for $m_\pi = 490$ MeV, and $G_M^*(0) \simeq 1.8$ for $m_\pi = 411$ MeV. These results are consistent with the estimates of the covariant spectator quark model with a regime where the meson and baryon masses used are those corresponding to the lattice QCD simulations [46,47].

Recall that the results described in this section include only the valence quark contributions. In this case we can conclude from Table III that the transitions $\gamma^* \Sigma^+ \to \Sigma^{*+}$ and $\gamma^* \Xi^0 \to \Xi^{*0}$ would give the same results in the limit that the octet (M_B) and decuplet ($M_{B'}$) baryon masses are, respectively, the same for the octet and decuplet members, or $M_\Sigma = M_\Xi$ and $M_{\Sigma^*} = M_{\Xi^*}$. The same argument holds also for the transitions $\gamma^* \Sigma^- \to \Sigma^{*-}$ and $\gamma^* \Xi^- \to \Xi^{*-}$.

The above relations can also be derived from the U-spin symmetry [9]. The U-spin symmetry implies that the systems are invariant in the exchange of a d and an s quark [6,9], or equivalently the symmetry in the same charge multiplet.

Another interesting limit is the exact $SU(3)$ symmetry limit, when $f_{i\pm}(Q^2) = f_{i0}(Q^2) \equiv f_i(Q^2)$ (f_i are independent of the flavors), and all the octet baryons have a unique mass M_B, and all the decuplet baryons have a unique mass $M_{B'}$. In this limit we expect no contributions for the reactions $\gamma^* \Sigma^- \to \Sigma^{*-}$ and $\gamma^* \Xi^- \to \Xi^{*-}$, because of $j_i^S \equiv 0$, and the same for all the other reactions, $j_i^S = \sqrt{2} f_i$, except for $\gamma^* \Sigma^0 \to \Sigma^{*0}$ with $j_i^S = \frac{\sqrt{2}}{2} f_i$ and $\gamma^* \Lambda \to \Sigma^{*0}$ with $j_i^S = \sqrt{\frac{3}{2}} f_i$. The suppression of the contributions for the $\gamma^* \Sigma^- \to \Sigma^{*-}$ and $\gamma^* \Xi^- \to \Xi^{*-}$ reactions compared to the others is also obtained with the U-spin symmetry [6,9]. Since in practice we break the $SU(3)$ symmetry using the physical masses, our estimates of the quark core contributions $\overline{G_M^b}(0)$ in Table IV can have variations of about up to 20%, similar to the amount of deviations in the masses.

The final result for the bare contributions given by (3.16) should also be corrected by a factor $\sqrt{Z_B}$ coming from the normalization of the octet baryon wave function due to the pion cloud effect. This normalization is necessary to describe the charge of the dressed baryon B. As explained in Refs. [34–36], the quark core contribution to the electric form factor is proportional to the factor $Z_B < 1$. Taking the proton as an example, the pion cloud contribution for the charge is $0.15 Z_N$ (contribution from the core of Z_N) in the model from Ref. [34], leading to $\sqrt{Z_N} = 0.93$, in order to reproduce the total proton charge. As for the decuplet wave functions, there are no corrections since the model used assumes that the pion cloud contributions are negligible [37]. We note that the effect of the octet wave function normalization is small since $\sqrt{Z_B} \simeq 1$; therefore, it does not affect the results appreciably. Thus, we use the simplest model, by setting $\sqrt{Z_B} = 1$. We will discuss the impact of this approximation later.

B. Pion cloud form factors

We discuss now the pion cloud contributions for the form factors. As before, we focus on the magnetic form factors.

Although the pion cloud dressing is included at the quark level effectively in the parametrization of the quark electromagnetic form factors, there are processes involving the pion cloud that are not taken into account. The processes in which a pion is exchanged between the different quarks cannot be represented by the quark dressing due to the pion cloud. Instead, the processes in which the pion is exchanged between different quarks are regarded as the pion is emitted and absorbed by the overall baryon in our model [35], which is represented by the diagram in Fig. 1.

We assume that the dominant contribution for the transitions comes from the direct coupling of the photon to the pion as depicted in Fig. 1, suggested by chiral perturbation theory [26]. As a consequence the pion cloud contributions for the $\gamma^* B \to B'$ transitions differ only by the quark flavor

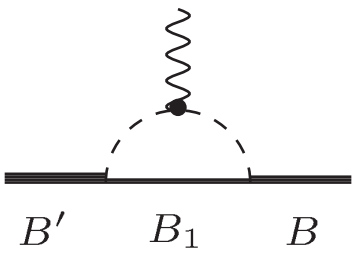

FIG. 1. Electromagnetic interaction with the pion (pion cloud contribution). Note that between the initial octet (B) and the final decuplet (B') baryon states, there can be several intermediate πB_1 states.

structure of the baryons and the kinematic effects due to the baryon masses. In the exact $SU(3)$ limit when all the octet baryon members have the same mass M_B and also all the decuplet baryon members have the mass $M_{B'}$, the pion cloud contribution will depend only on the flavor symmetry. Namely, the flavor effect can be determined using the $SU(3)$ meson-baryon couplings with the $SU(6)$ symmetry mixing parameter ratio, $\alpha \equiv D/(F+D) = 0.6$. Thus, assuming that the loop integrals arising from the diagram in Fig. 1 are only weakly dependent on the octet and decuplet baryon masses, the pion cloud contributions for all the octet to decuplet transitions can be estimated using the results obtained from the $\gamma^* N \to \Delta$ transition.

In summary, to estimate the pion cloud contributions for the $\gamma^* B \to B'$ transitions, we proceed as follows:

(i) Take a parametrization established for the pion cloud contributions for the $\gamma^* N \to \Delta$ transition.

(ii) Calculate the flavor corrections for the $\gamma^* B \to B'$ assuming that $M_B = M_N$ and $M_{B'} = M_\Delta$.

In the $\gamma^* N \to \Delta$ transition the pion cloud contributions can be represented by the phenomenological form [32]

$$G_M^\pi(Q^2) = \lambda_\pi \left(\frac{\Lambda_\pi^2}{\Lambda_\pi^2 + Q^2}\right)^2 (3G_D), \tag{3.19}$$

where $G_D = (1 + \frac{Q^2}{0.71})^{-2}$, with Q^2 in GeV^2, is the nucleon dipole form factor, λ_π is a coefficient associated with the strength of the pion cloud effect, and Λ_π a cutoff mass. The cutoff mass Λ_π controls the falloff of the pion cloud effects. Note that λ_π gives the relative contribution of the pion cloud to the total magnetic form factor for small Q^2, since for small Q^2, $G_M^*(Q^2) \approx 3G_D$, and $\lambda_\pi \approx \frac{G_M^\pi(Q^2)}{G_M^*(Q^2)}$.

To estimate the pion cloud dressing for the other octet to decuplet transitions, it is enough to calculate the flavor factor $f_{BB'}$ associated with the transition $\gamma^* B \to B'$ normalized by the transitions $\gamma^* N \to \Delta$ (or $\gamma^* p \to \Delta^+$) as shown next. The details are presented in Appendix C. Recalling that the strength of the pion cloud contribution for the $\gamma^* N \to \Delta$ reaction is given by the value λ_π at $Q^2 = 0$, the corresponding strength for the $\gamma^* B \to B'$ reaction can be obtained with the replacement

$$\lambda_\pi \to f_{BB'} \lambda_\pi. \tag{3.20}$$

Thus, the pion cloud contribution for the magnetic form factor in the reaction $\gamma^* B \to B'$ is

$$G_M^\pi(Q^2) = f_{BB'} \lambda_\pi \left(\frac{\Lambda_\pi^2}{\Lambda_\pi^2 + Q^2}\right)^2 (3G_D). \tag{3.21}$$

The factors $f_{BB'}$ are given in Table V. Note that with the above parametrization, we have the same Q^2 dependence for all $\gamma^* B \to B'$ reactions, which is a consequence of assuming the $SU(3)$ symmetry for the octet and decuplet baryon masses.

In the calculation we use the parametrization from Refs. [33,46]. Explicit values are $\lambda_\pi = 0.441$ and $\Lambda_\pi^2 = 1.53$ GeV^2. Although in Refs. [33,46] there are also higher angular momentum state contributions (D-states) aside from the S-state for the Δ baryon, the effects of those states are small. Therefore, the pion cloud parametrization given by Eq. (3.19) should be a very good approximation even when the D-states are neglected.

TABLE V. Coefficients $f_{BB'}$ associated with the $\gamma^* B \to B'$ transitions. The matrices J_3 and τ_3 are, respectively, the third component of the isospin-1 and isospin-1/2 operators.

	$f_{BB'}$
$\gamma^* N \to \Delta$	1
$\gamma^* \Lambda \to \Sigma^{*0}$	$\frac{2\sqrt{3}}{5}$
$\gamma^* \Sigma \to \Sigma^*$	$\frac{1}{5} J_3$
$\gamma^* \Xi \to \Xi^*$	$\frac{1}{5} \tau_3$

In summary, we calculate the magnetic transition form factors for the present model by

$$G_M^*(Q^2) = G_M^b(Q^2) + G_M^\pi(Q^2), \tag{3.22}$$

where G_M^b and G_M^π are defined respectively by Eqs. (3.16) and (3.21).

Note that $G_M^*(0)$ gives the transition magnetic moment in natural units. To convert $G_M^*(0)$ into the transition magnetic dipole moment $\mu_{BB'}$ in nuclear magneton ($\frac{e}{2M_N}$), we use [29]

$$\mu_{BB'} = \frac{M_N}{M_B} \sqrt{\frac{M_{B'}}{M_B}} G_M^*(0) \frac{e}{2M_N}. \tag{3.23}$$

IV. RESULTS

We divide our presentation of the results and analysis into four subsections. We start with the discussion of the numerical results for the transition form factors. Next, we focus on the symmetry relations among the different octet to decuplet transitions. Third, we compare the results with the available experimental information, in particular for the reactions aside from the $\gamma^* N \to \Delta$ reaction. Finally, we discuss the overall results.

A. Octet to decuplet electromagnetic transition form factors

The results of the transition form factors for the reactions $\gamma^* N \to \Delta$, $\gamma^* \Lambda \to \Sigma^{*0}$, $\gamma^* \Sigma \to \Sigma^*$, and $\gamma^* \Xi \to \Xi^*$ are presented, respectively, in Figs. 2–5. The results for $\gamma^* N \to \Delta$ represent those two reactions, $\gamma^* p \to \Delta^+$ and $\gamma^* \to \Delta^0$, which are equal in our model. The data are available only for the $\gamma^* p \to \Delta^+$ reaction. The calculations are based on the formulation exposed in the previous section, summarized by Eq. (3.22).

In Fig. 2 we present the result for the $\gamma^* N \to \Delta$ reaction, including the total, and the contributions from the bare core (valence quark), and the pion cloud, as well as the data for $\gamma^* p \to \Delta^+$ from DESY [62], SLAC [63], CLAS/Jefferson

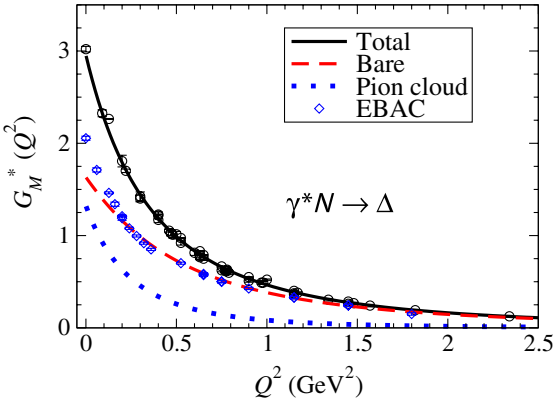

FIG. 2 (color online). Results for the $\gamma^* N \to \Delta$ transition. Data shown are for the $\gamma^* p \to \Delta^+$ reaction, from DESY [62], SLAC [63], CLAS/JLab [64], and MAID analysis [65,66]. Data for the large Q^2 region from CLAS/JLab are not included [77]. EBAC results are from Ref. [68].

Lab [64], and MAID analysis [65,66] for $Q^2 < 2.5$ GeV^2. Note that in the region $Q^2 < 2.5$ GeV^2, the agreement between the model result (solid line) and the data is excellent. This is because the Δ wave function in the model was calibrated previously to reproduce the data [33,46]. It should be mentioned, however, that the nucleon wave function used here is different from the one used in Refs. [33,46], but it was obtained from the study of the octet baryon electromagnetic form factors [34]. Although the pion cloud effects are included in the treatment of the baryon systems in Ref. [34] and not included in Refs. [33,46], both the nucleon wave functions yield very similar results.

Figure 2 also shows the insufficiency of the valence quark degrees of freedom only, to reproduce the magnetic form factor. Successful description of the reaction data was obtained using coupled channel reaction models (or dynamical models), where the meson-baryon interactions are taken into account, and the effect of the meson cloud dressing is included. Examples are the Sato-Lee model

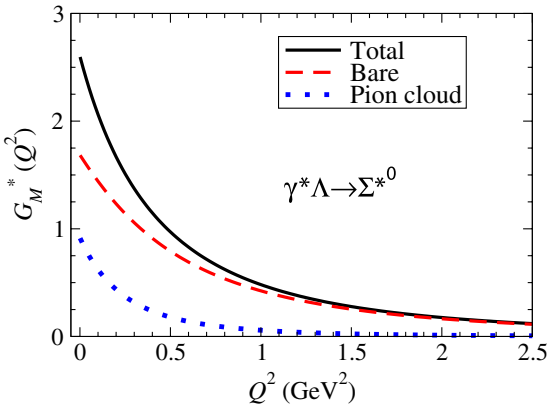

FIG. 3 (color online). Results for the $\gamma^* \Lambda \to \Sigma^{*0}$ transition.

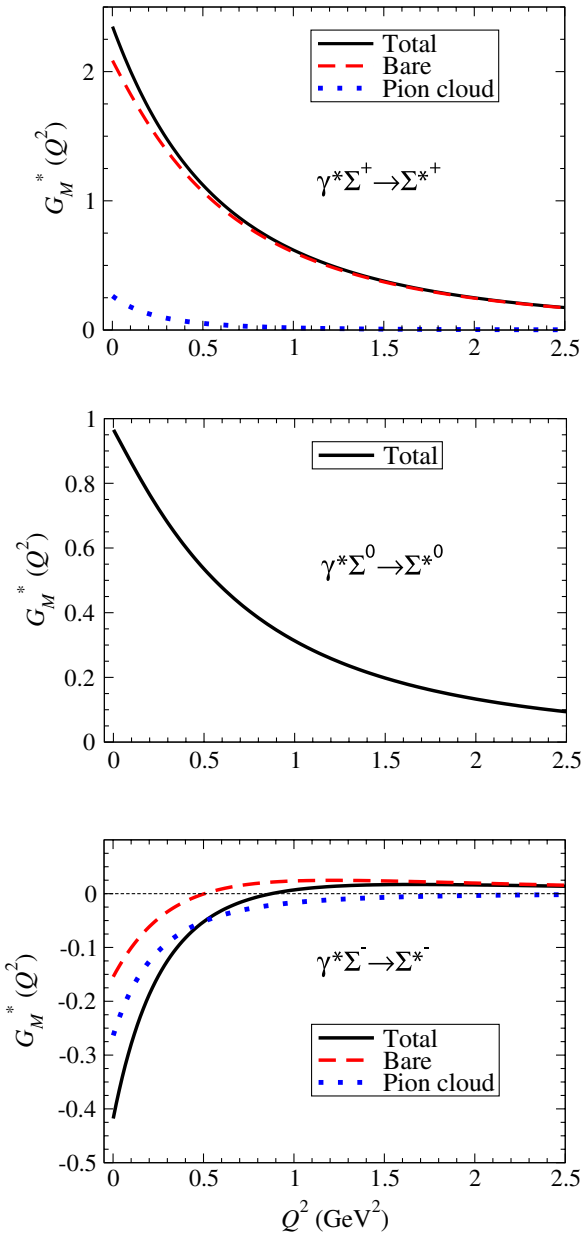

FIG. 4 (color online). Results for the $\gamma^* \Sigma^{\pm,0} \to \Sigma^{*\pm,0}$ reactions. For the Σ^0 case, the pion cloud contribution vanishes, and the bare and the total contributions are equal.

[67,68] and the Dubna-Mainz-Tapai model [69]. Also in these cases the pion cloud is about 30%–45% of the total. See Refs. [1,2] for a review.

Included also in Fig. 2 is the estimate of the quark core contributions from the EBAC group based on the Sato-Lee model [68]. The results are obtained using the Sato-Lee model, when the pion cloud contributions are removed. The good agreement between our bare result (dashed line) and the EBAC result, apart from the small deviation in the region $Q^2 < 0.2$ GeV^2, is an indication that our parametrization (3.19) gives a good representation of the pion cloud effects.

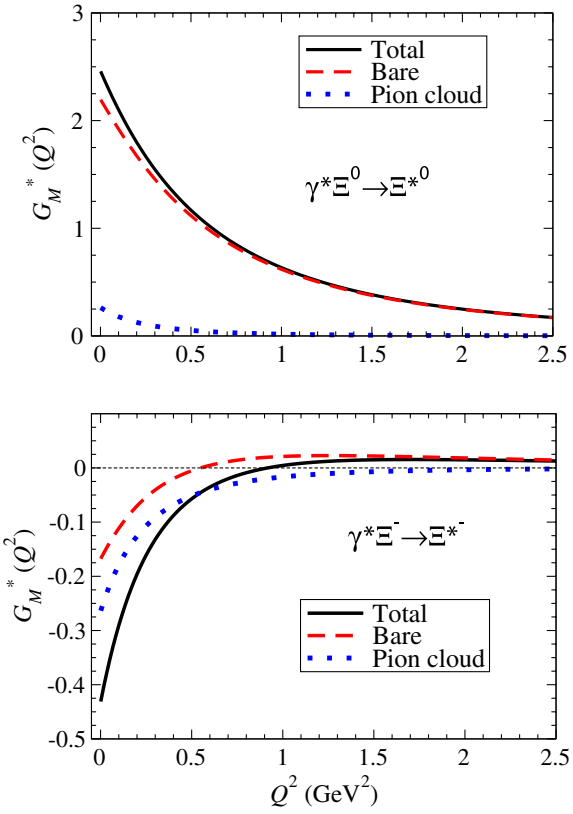

FIG. 5 (color online). Results for the $\gamma^*\Xi^{0,-}\to\Xi^{*0,-}$ reactions.

The results for G_M^*, together with the bare and the pion cloud contributions for $Q^2=0$, are presented in Table VI. The comparison of the bare, $G_M^b(0)$, with the upper limit, $\overline{G_M^b}(0)$, in Table IV allows us to conclude that the valence quark contribution in the model gives only about 80%–90% of the maximum value.

In Fig. 3 one can see the dominance of the valence quark (bare) contribution in the $\gamma^*\Lambda\to\Sigma^{*0}$ reaction. This feature is expected based on the estimate of the pion cloud contribution: about 0.92 at $Q^2=0$, smaller than the one for the $\gamma^*N\to\Delta$ transition of 1.32 as shown in Table IV.

TABLE VI. Results for $G_M^*(0)$. Values for $|G_M^*(0)|_{\rm exp}$ are estimated by Eq. (4.1), using the experimental values of $\Gamma_{B'\to\gamma B}$.

	$G_M^b(0)$	$G_M^\pi(0)$	$G_M^*(0)$	$\lvert G_M^*(0)\rvert_{\rm exp}$
$\gamma^*p\to\Delta^+$	1.63	1.32	2.95	3.04 ± 0.11 [4]
$\gamma^*n\to\Delta^0$	1.63	1.32	2.95	3.04 ± 0.11 [4]
$\gamma^*\Lambda\to\Sigma^{*0}$	1.68	0.92	2.60	3.35 ± 0.57 [4]
$\gamma^*\Sigma^+\to\Sigma^{*+}$	2.09	0.26	2.35	4.10 ± 0.57 [5]
$\gamma^*\Sigma^0\to\Sigma^{*0}$	0.97	0.00	0.97	
$\gamma^*\Sigma^-\to\Sigma^{*-}$	−0.15	−0.26	−0.42	<0.8 [8]
$\gamma^*\Xi^0\to\Xi^{*0}$	2.19	0.26	2.46	
$\gamma^*\Xi^-\to\Xi^{*-}$	−0.17	−0.26	−0.43	

As for the $\gamma^*\Sigma^{\pm,0}\to\Sigma^{*\pm,0}$ reactions, one can observe in Fig. 4 different trends by the Σ charges. For the reaction with the Σ^+, the result is comparable to that of the $\gamma^*N\to\Delta$, while one has a smaller magnitude of about 50% for the reaction with the Σ^0, and an even smaller magnitude for the reaction with the Σ^-. In these reactions the magnitude of the pion cloud contributions is small—0.26 at $Q^2=0$ (about 20% of the $\gamma^*N\to\Delta$ reaction) for the reactions with the $\Sigma^\pm$—and vanishes for the reaction with the Σ^0.

The results for the $\gamma^*\Xi^{0,-}\to\Xi^{*0,-}$ reactions are presented in Fig. 5. They are similar to the results described for the $\gamma^*\Sigma^+\to\Sigma^{*+}$ and $\gamma^*\Sigma^-\to\Sigma^{*-}$, respectively, for the reactions with the Ξ^0 and Ξ^- in the initial states.

In Figs. 2–5, we can observe the fast falloff of the pion cloud contributions and the dominance of the valence quark contributions with increasing Q^2. For a very large Q^2, one has $G_M^*\propto 1/Q^4$ according to Eq. (3.16), in agreement with pQCD estimates [32,70]. The pion cloud contributions given by Eq. (3.21) vary as $G_M^\pi\propto 1/Q^8$.

We now comment on the effects due to the baryon wave function normalization. As mentioned already, only the octet baryon wave functions are subject to be modified in the present treatment, by the factor $\sqrt{Z_B}$ in the valence quark contributions. The effect of the normalization is in general small, since $\sqrt{Z_B}\simeq 1$ ($\sqrt{Z_\Lambda}=0.965$, $\sqrt{Z_\Sigma}=0.958$ and $\sqrt{Z_\Sigma}=0.997$), except for the core contribution for the $\gamma^*N\to\Delta$ transition with a 7% correction ($\sqrt{Z_N}=0.931$). In this case, however, the effect in the total magnitude of the form factor is about 3%, because the correction affects only the bare contribution and the pion cloud contribution is significant (44%). Thus, we conclude that the corrections due to the normalization of the baryon wave functions are small (order of a few percent) and can be neglected in a first approximation.

B. Symmetry between different transitions

Roughly, we can classify the results for the $\gamma^*B\to B'$ transition form factors according to the magnitudes of magnetic dipole form factor G_M^*,

large: $\gamma^*N\to\Delta$, $\gamma^*\Lambda\to\Sigma^{*0}$,
$\gamma^*\Sigma^+\to\Sigma^{*+}$, $\gamma^*\Xi^0\to\Xi^{*0}$,
moderate: $\gamma^*\Sigma^0\to\Sigma^{*0}$,
small: $\gamma^*\Sigma^-\to\Sigma^{*-}$, $\gamma^*\Xi^-\to\Xi^{*-}$.

This classification has an implication for the magnitude of the decay widths, as we will see in the next section.

The observed magnitudes for G_M^* mainly reflect the dominant valence quark structure, although modified by the effect of the pion cloud. As mentioned in Sec. III A based on Table III, except for the deviations due to the mass differences, we can expect similar results for the $\gamma^*\Sigma^+\to\Sigma^{*+}$ and $\gamma^*\Xi^0\to\Xi^{*0}$ transitions. The same holds for the reactions $\gamma^*\Sigma^-\to\Sigma^{*-}$ and $\gamma^*\Xi^-\to\Xi^{*-}$.

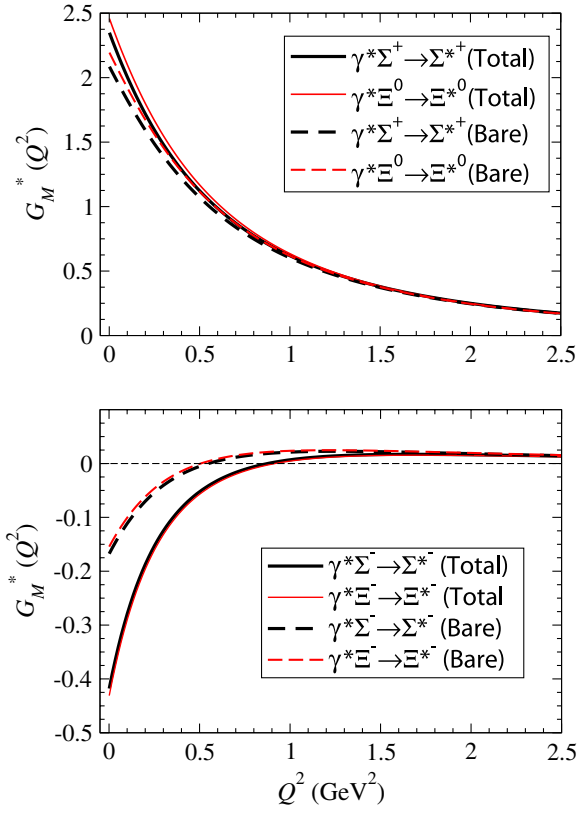

FIG. 6 (color online). Comparison between the $\gamma^*\Sigma^+ \to \Sigma^{*+}$ and $\gamma^*\Xi^0 \to \Xi^{*0}$ reactions (top) and between the $\gamma^*\Sigma^- \to \Sigma^{*-}$ and $\gamma^*\Xi^0 \to \Xi^{*0}$ reactions (bottom).

We compare the results for these reactions directly in Fig. 6.

Note in Fig. 6 the closeness between the results for the two reactions, both for the bare (dashed lines) and the total (solid lines). These results are the consequences of the following two effects: similarity in the valence quark structure and identical contribution from the pion cloud contributions (see Table V). Concerning the valence quark contributions, the similarity in the results of the two reactions is a combination of the identical transition current coefficients (j_i^S) and the kinematics. In fact, although the mass configurations are different for the $\gamma^*\Sigma \to \Sigma^*$ and $\gamma^*\Xi \to \Xi^*$ reactions, the transition three-momentum $|\mathbf{q}|$ at $Q^2 = 0$ in the baryon B' rest frame, are almost the same, 0.18 and 0.20 GeV, respectively.

The difference in magnitude between the two sets, ($\gamma^*\Sigma^+ \to \Sigma^{*+}$, $\gamma^*\Xi^0 \to \Xi^{*0}$) and ($\gamma^*\Sigma^- \to \Sigma^{*-}$, $\gamma^*\Xi^- \to \Xi^{*-}$), in our model is a consequence of the approximate $SU(3)$ symmetry. Furthermore, as commented in Sec. III A, a model with the exact $SU(3)$ symmetry limit would give no contribution for the last two reactions. In contrast, the small violation of the symmetry, in particular in the $SU(2)$ sector, due to the asymmetry between the isoscalar and isovector quark form factors $f_\pm(Q^2)$, is the reason why the present model is successful in the description of the neutron electric form factor [34,35,39]. In other approaches the small magnitudes of the G_M^* results for the $\gamma^*\Sigma^- \to \Sigma^{*-}$ and $\gamma^*\Xi^- \to \Xi^{*-}$ reactions can be a consequence of U-spin symmetry [9].

We can also study the relation between the transitions $\gamma^*N \to \Delta$ and $\gamma^*\Lambda \to \Sigma^{*0}$ based on the similarity suggested by the valence quark structure given in Table III. From Table III, we may conclude that the transition form factors between the $\gamma^*\Lambda \to \Sigma^{*0}$ and $\gamma^*N \to \Delta$ reactions differ by a factor of $\sqrt{\frac{3}{4}}$, if only the valence quark contributions are considered. We examine this in Fig. 7 by comparing the form factor of $\gamma^*N \to \Delta$ with that of $\gamma^*\Lambda \to \Sigma^{*0}$ multiplied by $\sqrt{\frac{4}{3}}$. However, the results must be interpreted with care. Focusing on the final results (total, solid lines), the similarity between the results for the two reactions is an accidental combination of a large pion cloud effect and a smaller core contribution for the $\gamma^*N \to \Delta$ reaction and the opposite, a smaller pion cloud effect and a larger core contribution for the $\gamma^*\Lambda \to \Sigma^{*0}$ reaction. The symmetry properties should be better observed in the bare contributions (dashed lines). In fact, the two dashed lines have a similar shape but differ in magnitude by about 20% near $Q^2 = 0$. This is a consequence of the differences in the masses and radial wave functions.

Then, we conclude that the closeness between the total results for the $\gamma^*N \to \Delta$ and $\gamma^*\Lambda \to \Sigma^{*0}$ reactions, also predicted by the U-spin symmetry, is accidental, since the pion cloud contributions should break the symmetry appreciably. In fact, for the $\gamma^*N \to \Delta$ reaction, the pion cloud contribution is 80% of the quark core contribution, while in the $\gamma^*\Lambda \to \Sigma^{*0}$ reaction, the pion contribution is 55%. Note that the U-spin symmetry takes into account only the valence quark contributions of the baryons. If it is applied also for the meson cloud contributions, one must assume the same proportionality between the meson cloud and valence quark contributions.

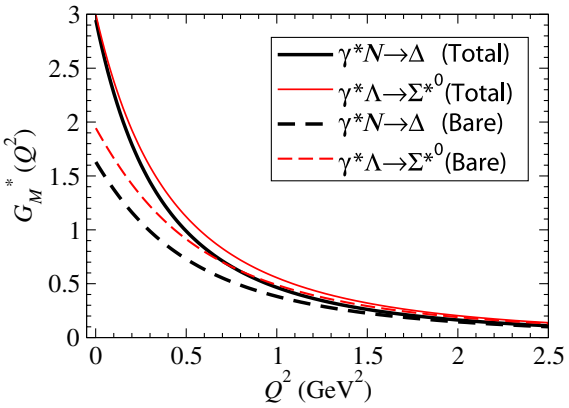

FIG. 7 (color online). Comparison of the reactions $\gamma^*N \to \Delta$ and $\gamma^*\Lambda \to \Sigma^{*0}$. The results for $\gamma^*\Lambda \to \Sigma^{*0}$ are multiplied by the factor $\sqrt{\frac{4}{3}}$.

C. Decay widths

We now discuss the results for the $B' \to \gamma B$ decay widths, which is closely connected with $|G_M^*(0)|$, as we show next. Therefore, the discussion about the decay widths is nearly equivalent to the discussion of the magnitudes, $|G_M^*(0)|$. Note, however, that only the decay widths for the reactions, $\gamma^* N \to \Delta$, $\gamma^* \Lambda \to \Sigma^0$, and $\gamma^* \Sigma^+ \to \Sigma^+$ are experimentally determined.

Assuming the G_M^* dominance (G_E^*, $G_C^* \simeq 0$), we can calculate the decay width $\Gamma_{B' \to \gamma B}$ by [29,71,72]

$$\Gamma_{B' \to \gamma B} = \frac{\alpha}{16} \frac{(M_{B'}^2 - M_B^2)^3}{M_{B'}^3 M_B^2} |G_M^*(0)|^2, \qquad (4.1)$$

where $\alpha = \frac{e^2}{4\pi} \simeq \frac{1}{137}$ is the electromagnetic fine structure constant.

The assumption of the G_M^* dominance for $Q^2 = 0$ is justified when $|G_E^*(0)|$ is small enough, e.g., it is an order of a few percent of $|G_M^*(0)|$. Then, since the correction to the term $|G_M^*(0)|^2$ in Eq. (4.1) enters as $|G_M^*(0)|^2 + 3|G_E^*(0)|^2$, we may neglect the $G_E^*(0)$ with an accuracy of about 1%. This is indeed supported by the different estimates for $G_E^*(0)$ [15,21,22,25,29].

Estimates of $G_M^*(0)$ based on Eq. (4.1) are presented in Table VI, together with our predictions for $G_M^*(0)$. Notice, in particular, the result for the $\gamma^* N \to \Delta$ reaction, $G_M^*(0) = 3.04 \pm 0.11$, is very close to the experimental value of $G_M^*(0) = 3.02 \pm 0.03$ [65]. In Table VI we can see that our results for $\gamma^* \Lambda \to \Sigma^{*0}$ and $\gamma^* \Sigma^+ \to \Sigma^{*+}$ underestimate the values of $|G_M^*(0)|$, determined from the data. In fact our results give only 78% and 57%, respectively, compared with the corresponding experimental central values (underestimates of 1.3 and 3.1 standard deviations, respectively). We will discuss the impact of these results in more detail later.

In the S-state approximation with $G_E^* = 0$, we can also calculate the helicity amplitudes $A_{3/2}$ and $A_{1/2}$ in terms of G_M^* using the relations $A_{3/2} = -\sqrt{3} F G_M^*$ and $A_{1/2} = -F G_M^*$, where the factor F is a given function of Q^2 [49,73]. For $Q^2 = 0$, the factor F is given by $F = \frac{e}{4M_B} \sqrt{\frac{M_{B'}^2 - M_B^2}{2M_B}}$. In Table VII we present the results for the helicity amplitudes $A_{3/2}$ and $A_{1/2}$ for $Q^2 = 0$, calculated in the approximation $G_E^* = 0$. Finally, we also present our predictions for the decay widths calculated by Eq. (4.1). The results are compared with the available experimental results for $\Gamma_{B' \to \gamma B}$ ($\Gamma_{\rm exp}$).

Our results for the decay widths in Table VII are comparable with most of the predictions presented in the literature [11–15,17,20–24,27,65]. The exception is the result for the $\Delta \to \gamma N$ reaction, where most of the models underestimate the experimental data by more than 200 keV [11,14,15,17,21,22,28], except for the heavy baryon chiral perturbation theory (HBχPT) [24], large N_c limit [27], and QCD sum rules [23].

Estimates for the $\Sigma^{*0} \to \gamma \Lambda$ decay width are in the range 150–300 keV for a large variety of quark models, algebraic models of hadron structure, Skyrme, and soliton models [11–15,17,20–22]. Only HBχPT has a window 252–540 keV [24], while the large N_c limit predicts 336 ± 81 keV [27] and may overestimate the result of 300 keV, as well as the QCD sum rules with 409 keV [23]. Our result, 284 keV, underestimates the experimental value from Ref. [4] by 1.2 standard deviations, and also that from Refs. [5,6] by 1.6 standard deviations.

As for the $\Sigma^{*+} \to \gamma \Sigma^+$ decay width, most of the predictions are in the range 50–110 keV, with the following exceptions: QCD sum rules (150 keV) [23], an algebraic model of hadron structure (141 keV) [28], HBχPT (70–220 keV) [24], and large N_c limit (140 ± 36 keV) [27]. Overall, these estimates are considerably smaller than the experimental result of 250 ± 70 keV [5], except for HBχPT [24]. Our estimate, 82 keV, underestimates the data more than 2.4 standard deviations.

As for the remaining reactions, no experimental data are available, and the decay widths we have obtained, are comparable with those calculated by the several theoretical models. In particular, the $\Xi^{*0} \to \gamma \Xi^0$ decay width is close to the $\Sigma^{*+} \to \gamma \Sigma^+$ result (82 keV versus 101 keV, in our case); the $\Sigma^{*0} \to \gamma \Sigma^0$ decay width (14 keV) is about an order of magnitude smaller than that for $\Sigma^{*+} \to \gamma \Sigma^+$; and the results for $\Sigma^{*-} \to \gamma \Sigma^-$ and $\Xi^{*-} \to \gamma \Xi^-$ are reduced to a few keV (2.6 and 3.6 keV, in our case).

Concerning the $\gamma^* \Lambda \to \Sigma^{*0}$ and $\gamma^* \Sigma^+ \to \Sigma^{*+}$ decay widths, they can also be compared with the estimates made based on the U-spin symmetry. The U-spin symmetry relates the $\gamma^* \Lambda \to \Sigma^{*0}$ and $\gamma^* \Sigma^+ \to \Sigma^{*+}$ reactions with the $\gamma^* N \to \Delta$ reaction. One can then make predictions for the $\gamma^* \Lambda \to \Sigma^{*0}$ and $\gamma^* \Sigma^+ \to \Sigma^{*+}$ reactions using the experimental results for $\gamma^* N \to \Delta$. Assuming that the U-spin symmetry holds for the $|G_M^*(0)|$, we obtain using Eq. (4.1), 292 ± 27 keV for $\gamma^* \Lambda \to \Sigma^{*0}$ and 138 ± 13 keV for $\gamma^* \Sigma^+ \to \Sigma^{*+}$. Note the closeness of the result for $\gamma^* \Lambda \to \Sigma^{*0}$ with our result. The difference is 0.8 standard deviations. As for the $\gamma^* \Sigma^+ \to \Sigma^{*+}$ reaction, our prediction, 82 keV, underestimates the U-spin symmetry estimate

TABLE VII. Results for $G_M^*(0)$, helicity amplitudes $A_{3/2}(0)$ and $A_{1/2}(0)$ in 10^{-3} GeV$^{-1/2}$ and decay widths $\Gamma_{B' \to \gamma B}$ in keV.

	$G_M^*(0)$	$A_{3/2}(0)$	$A_{1/2}(0)$	$\Gamma_{B' \to \gamma B}$	$\Gamma_{\rm exp}$
$\gamma^* p \to \Delta^+$	2.95	−240	−139	620	660 ± 47 [4]
$\gamma^* n \to \Delta^0$	2.95	−240	−139	620	660 ± 47 [4]
$\gamma^* \Lambda \to \Sigma^{*0}$	2.60	−168	−97	284	470 ± 160 [4]
					445 ± 102 [5,6]
$\gamma^* \Sigma^+ \to \Sigma^{*+}$	2.35	−118	−68	82	250 ± 70 [5]
$\gamma^* \Sigma^0 \to \Sigma^{*0}$	0.97	−48	−28	14	
$\gamma^* \Sigma^- \to \Sigma^{*-}$	−0.42	21	12	2.6	<9.5 [8]
$\gamma^* \Xi^0 \to \Xi^{*0}$	2.46	−118	−68	101	
$\gamma^* \Xi^- \to \Xi^{*-}$	−0.43	21	12	3.1	

by 4.3 standard deviations as a consequence of the small errorbar, although the result deviates only about 41% from the central value.

A comment on the U-spin symmetry estimates made for the same reactions in Ref. [6] is in order. Those estimated values are in close agreement with the experimental results. We note, however, that the estimates in Ref. [6] were based on the U-spin symmetry between the helicity amplitudes and not between the form factors $G_M^*(0)$ as discussed previously in our case. The difference in both estimates are the mass factors included in the coefficient, $F = \frac{e}{4M_B}\sqrt{\frac{M_{B'}|\mathbf{q}|}{M_B}}$, which transforms form factors into helicity amplitudes.

D. Discussion

The interpretation of the gap between our results for the decay widths and the experimental ones can be more easily made using $G_M^*(0)$, assuming that G_M^* is the dominant form factor. As discussed already, the G_M^* dominance is indeed a good approximation.

Based on the upper limits for the bare results $G_M^b(0)$ given in Table IV represented as $\overline{G_M^b}(0)$, we can conclude that the core contribution is at most 2.0 for $\gamma^*\Lambda \to \Sigma^{*0}$ and 2.3 for $\gamma^*\Sigma^+ \to \Sigma^{*+}$. These limits are the consequence of the normalization of the baryon wave functions and cannot be exceeded if only the valence quark degrees of freedom are considered. In the following, we assume that the experimental sign of $G_M^*(0)$ is the same as $G_M^b(0)$. In Table VI comparing our results with the experimental estimates of 3.35 and 4.10, respectively, for $\gamma^*\Lambda \to \Sigma^{*0}$ and $\gamma^*\Sigma^+ \to \Sigma^{*+}$, one can conclude that about 1.35 ± 0.57 for the former, and 1.80 ± 0.57 for the latter, should be a consequence of other effects than the valence quarks, such as the pion (or meson) cloud effects. However, our present estimate of the pion cloud effects is very small for the $\gamma^*\Sigma^+ \to \Sigma^{*+}$ reaction (only 0.26), leading to a noticeable underestimate of the experimental value of 4.1 ± 0.6. The necessary amount of the pion cloud would be then 1.8 ± 0.6, where the lower limit 1.2 is roughly the same amount of the pion cloud in the $\gamma^*N \to \Delta$ reaction. This minimum amount necessary is much larger than the 0.26 of our present estimate. Furthermore, notice that the above estimate is made using the upper limit value for $G_M^b(0)$, which is independent of the radial wave functions. If we use the values for $G_M^b(0)$ given in Table VI, the amount of the missing meson cloud contribution should be even larger (2.0 ± 0.6 for the $\gamma^*\Sigma^+ \to \Sigma^{*+}$ case).

Then, we conclude that even larger pion or other meson cloud contributions are necessary to explain the $\gamma^*\Sigma^+ \to \Sigma^{*+}$ data, in particular the decay width. We emphasize that this conclusion is not only restricted to our model, but can also be inferred from a large variety of theoretical models. As mentioned already, typical predictions for the $\Sigma^{*+} \to \gamma\Sigma^+$ decay width are in the 50–110 keV range, where the more optimistic estimates differ from the experimental value by 2 standard deviations. Similarly, the U-spin symmetry estimate differs by 1.6 standard deviations.

Therefore, the study of the $\gamma^*B \to B'$ reactions requires more elaborated investigations. A possible effect to rescue the shortage of the present result for $\Sigma^{*+} \to \gamma\Sigma^+$ decay width, and not yet included in our model, is the kaon cloud contributions. Although the contributions may be negligible for the $\gamma^*N \to \Delta$ reaction, the kaon cloud effects are expected to be larger in the $\gamma^*\Xi^{0,-} \to \Xi^{*0,-}$ reactions and can also be important for the $\gamma^*\Sigma^{0,\pm} \to \Sigma^{*0,\pm}$ reactions, because of the strangeness.

A simple estimate based on the exact $SU(3)$ symmetry predicts that the kaon cloud cloud contribution is $1/6$ of the pion cloud contribution for the $\gamma^*N \to \Delta$ reaction. The same estimate for the $\gamma^*\Sigma^+ \to \Sigma^{*+}$ reaction gives a kaon cloud contribution five times larger than that of the pion cloud in this limit, which increases the total meson cloud contributions (pion plus kaon) to the same amount of the $\gamma^*N \to \Delta$ transition. This enhancement of the meson cloud contributions would increase our estimate for the $\Sigma^{*+} \to \gamma\Sigma^+$ decay width for a value compatible with the experimental result. Note, however, the $SU(3)$ symmetry is broken in nature; namely, the kaon is heavier than the pion, and the kaon cloud contribution should be smaller than the estimate based on the $SU(3)$ symmetry. Nevertheless, it is worth noting that the kaon cloud contribution should increase our result and lead to a better agreement with the data. The kaon cloud correction affects also the $\gamma^*\Xi^{0,-} \to \Xi^{*0,-}$ reactions, and in a smaller amount the $\gamma^*N \to \Delta$ reaction.

A more realistic estimate of the kaon cloud contributions for the electromagnetic transition form factors, including explicitly the dependence on the masses of the kaon, the octet, and decuplet baryons, is a very promising topic of investigation for the future. Such a study may help to explain the decuplet decay widths, but it is beyond the scope of the present work. In this exploratory study, we have focused on the valence quark and the pion cloud contributions.

In summary, the present study suggests that the meson cloud effects, besides the pion cloud, are important in the $\gamma^*B \to B'$ reactions, in particular for those involving the Σ^* in the final states. As pointed out already in Refs. [5,6], meson cloud effects may be indispensable to explain the data. In fact, lattice QCD simulations, quark models, and others generally underestimate the magnitude of the form factors extracted from the data. Even the models with the pion cloud effects [17,20–22] fail to reproduce the magnitude for the $\gamma^*\Lambda \to \Sigma^{*0}$ and $\gamma^*\Sigma^+ \to \Sigma^{*+}$ form factors. The estimates from HBχPT, where the kaon cloud was taken into account, support also the relevance of the kaon cloud effects [24]. The quantitative estimates for the decay widths from HBχPT (252–540 keV for $\gamma^*\Lambda \to \Sigma^{*0}$ and 70–220 keV for $\gamma^*\Sigma^+ \to \Sigma^{*+}$) are, however, too broad to

draw more definite conclusions. More accurate estimates of the kaon cloud effects may help to explain the gap existing between the predictions and the data.

In order to clarify and improve the present situation, new experimental determinations of the decuplet to octet radiative decay widths would be very useful. Of critical importance is to confirm (or deny) the result for the $\Sigma^{*+} \to \gamma\Sigma^{+}$ decay width. The determination of the other decuplet baryon radiative decay widths can also be important. For instance, the determination of the $\Sigma^{*0} \to \gamma\Sigma^{0}$ decay width would be an excellent test for theoretical models, in particular to clarify the role of the meson cloud, since the valence quark contribution is expected to be very small. Another interesting case would be the determination of the $\Xi^{*0} \to \gamma\Xi^{0}$ decay width, because it is expected to be close to that of $\Sigma^{*+} \to \gamma\Sigma^{+}$ in our model, and also according to the U-spin symmetry.

V. SUMMARY AND CONCLUSIONS

In this work we have studied the octet to decuplet baryon electromagnetic transitions using the covariant spectator quark model, and predicted the magnetic dipole form factors for the reactions with strange baryons. In the present study we have adopted well established parametrizations for the octet and decuplet baryon wave functions developed in the previous works. Our estimates of the valence quark contributions for the transition form factors are based on the assumption that the quark-diquark S-state is the dominant configuration in the baryon systems. Our results are consistent with lattice QCD simulations and those of other quark models. Based on the $SU(3)$ symmetry for the meson-baryon couplings, we have extended the calculation of the pion cloud contributions for the $\gamma^{*}N \to \Delta$ reaction to the remaining $\gamma^{*}B \to B'$ reactions with strange baryons.

It would also be very interesting to go beyond the S-state approximation and estimate the quadrupole form factors. However, except for the Δ case, one has no reliable parametrization at the moment for the small D-state components in the decuplet baryon wave functions, which yield the contributions for those form factors [33,37,46]. Nevertheless, the contributions from such small components are expected to be only of the order of a few percent compared to the magnetic dipole form factor.

It is shown that the covariant spectator quark model is very useful to estimate the valence quark contributions for the $\gamma^{*}B \to B'$ transition form factors, since, in particular, it provides an upper limit of the valence quark contributions independent of the details of the baryon radial wave functions, that can be used to infer the magnitude of other contributions besides the valence quark contributions. In particular, the estimate of the valence quark contribution for the $\gamma^{*}N \to \Delta$ reaction is very important to understand why the pion cloud, or meson cloud in general, is of fundamental importance to obtain a consistent description of the experimental data.

When compared with the available experimental data (including the $\gamma^{*}\Lambda \to \Sigma^{*0}$ and $\gamma^{*}\Sigma^{+} \to \Sigma^{*+}$ reactions), we have found that the valence quark plus pion cloud contributions are insufficient to explain the data. This shortcoming is particularly evident for the $\gamma^{*}\Sigma^{+} \to \Sigma^{*+}$ reaction. Namely, our result underestimates the experimental radiative decay width by 2.4 standard deviations. Since the effect of the valence quark core is bounded by an upper limit, we interpret the underestimates of the present study as a consequence of the smallness of the meson cloud contributions in the model, where we have included explicitly only the effect of the lightest meson, the pion in this exploratory study where it is generally believed to be dominant.

Our results strongly suggest the potential importance of including clouds of mesons heavier than the pion in the $\gamma^{*}B \to B'$ transitions with strange baryons, especially the kaon cloud. A simple estimate based on the $SU(3)$ symmetry, using the same mass and couplings for the kaon and pion, indicates that the meson cloud contributions, pion plus kaon clouds, are expected to increase the magnitude for the $\Sigma^{*+} \to \gamma\Sigma^{+}$ form factors and improve the present result towards the experimental one. As the $SU(3)$ symmetry is broken in practice, we conclude that a more elaborate and consistent study for the meson cloud dressing is necessary in order to understand better the $\gamma^{*}B \to B'$ data.

Finally, we emphasize again that more experimental data for the octet to decuplet baryon transitions, $\gamma^{*}B \to B'$, are desired to clarify the present situation and shed light on the reaction mechanisms.

ACKNOWLEDGMENTS

We thank R. Wilson for helping with proofreading. G. R. was supported by the Fundação para a Ciência e a Tecnologia under Grant No. SFRH/BPD/26886/2006. The authors also would like to thank the International Institute of Physics, Federal University of Rio Grande do Norte, Brazil, where the revision of the manuscript was completed. This work was supported by Portuguese national funds through FCT—Fundação para a Ciência e a Tecnologia, under Grant No. PTDC/FIS/113940/2009, "Hadron Structure with Relativistic Models," and Project No. PEst-OE/FIS/UI0777/2011. This work was also supported partially by the European Union under the HadronPhysics3 Grant No. 283286, (K. T.), the University of Adelaide, and the Australian Research Council through Grant No. FL0992247.

APPENDIX A: DECUPLET SELF ENERGY

In this Appendix we describe the formalism on the decuplet self-energy and its relation to the decuplet baryon masses.

TABLE VIII. Pion-baryon couplings in $SU(3)$ symmetry with $\alpha \equiv D/(F+D) = 0.6$. Here ξ_π and ξ_Σ are the isospin-1 polarization vectors of the π and Σ, $\boldsymbol{\tau}$ are the isospin-1/2 matrices, $\mathbf{T}$ are the isospin $1/2$ to $3/2$ transition operator matrices, $\mathbf{J}$ are the isospin-1 matrices, and $\mathbf{t}$ are the isospin $3/2$ matrices. For the diagonal operators, the isospin wave functions of the initial and final baryons are suppressed.

$\pi BB'$	$\mathcal{O}_{\pi BB'}$	$g_{\pi BB'}$
πNN	$g_{\pi NN}(\xi_\pi^* \cdot \boldsymbol{\tau})$	g
$\pi\Lambda\Sigma$	$g_{\pi\Lambda\Sigma}(\xi_\pi^* \cdot \xi_\Sigma)$	$\frac{2\sqrt{3}}{5} g$
$\pi\Sigma\Sigma$	$g_{\pi\Sigma\Sigma}(\xi^* \cdot \mathbf{J})$	$\frac{4}{5} g$
$\pi\Xi\Xi$	$g_{\pi\Xi\Xi}(\xi_\pi^* \cdot \boldsymbol{\tau})$	$-\frac{1}{5} g$
$\pi N\Delta$	$g_{\pi N\Delta}(\xi_\pi^* \cdot \mathbf{T})$	$\frac{2\sqrt{2}}{5} g$
$\pi\Lambda\Sigma^*$	$g_{\pi\Lambda\Sigma^*}(\xi_\pi^* \cdot \xi_{\Sigma^*})$	$\frac{2}{5} g$
$\pi\Sigma\Sigma^*$	$g_{\pi\Sigma\Sigma^*}(\xi_\pi^* \cdot \mathbf{J})$	$\frac{2\sqrt{6}}{15} g$
$\pi\Xi\Xi^*$	$g_{\pi\Xi\Xi^*}(\xi_\pi^* \cdot \boldsymbol{\tau})$	$\frac{2}{5} g$
$\pi\Delta\Delta$	$g_{\pi\Delta\Delta}(\xi_\pi^* \cdot \mathbf{t})$	g
$\pi\Sigma^*\Sigma^*$	$g_{\pi\Sigma^*\Sigma^*}(\xi_\pi^* \cdot \mathbf{J})$	$\frac{2\sqrt{2}}{\sqrt{15}} g$
$\pi\Xi^*\Xi^*$	$g_{\pi\Xi^*\Xi^*}(\xi_\pi^* \cdot \boldsymbol{\tau})$	$\frac{1}{\sqrt{5}} g$

The decuplet baryon B' mass can be decomposed as $M_{B'} = M_{0B'} + \Sigma_0^*(M_{B'})$, where Σ_0^* is the baryon self-energy at the pole position. Considering only the pion cloud excitations, we can represent the self-energy as $\Sigma_0^* = G_{1B'}\mathcal{B}_1 + G_{2B'}\mathcal{B}_2$, where $\mathcal{B}_1$ and $\mathcal{B}_2$ are the value of the Feynman integrals, respectively, with an intermediate octet and decuplet baryons, where the factors G_{1B} and G_{2B} are the coupling factors for the corresponding pion loops. Using the couplings in Table VIII, we obtain the factors listed in Table IX. As there are no pion cloud contributions for the Ω^- baryon, $M_\Omega = M_{0B'}$.

APPENDIX B: OVERLAP INTEGRAL

In this Appendix we discuss the properties of the integral $\mathcal{I}(Q^2)$ given by Eq. (3.10), also called body integral [32], for $Q^2 = 0$. The value of $\mathcal{I}(0)$ measures the degree of superposition of the radial wave functions $\psi_{B'}$ and ψ_B, when $Q^2 = 0$.

In this Appendix we show that

$$\mathcal{I}(0) \leq 1, \tag{B1}$$

where the equality holds only for the case $M_{B'} = M_B$.

Even in the equal mass case it is not assured that $\mathcal{I}(0) = 1$, unless $\psi_{B'} \equiv \psi_B$. We can expect, however, in the equal mass case, $\mathcal{I}(0) \simeq 1$, if the two radial functions are very similar.

Next, we explicitly demonstrate the relation (B1). In Sec. B 1 (Part 1) we explain the basic steps of the demonstration, while in Sec. B 2 (Part 2), we present the more technical details.

1. Part 1

The integral $\mathcal{I}(0)$ is covariant, therefore the result is independent of the frame. For simplicity, we use the B' rest frame.

In the B' rest frame, one can write the initial (P_-) and final (P_+) momenta, choosing z as the photon direction (momentum $\mathbf{q}$) as

$$P_+ = (M_{B'}, 0, 0, 0), \qquad P_- = (E_B, 0, 0, -|\mathbf{q}|), \qquad q = (\omega, 0, 0, |\mathbf{q}|), \tag{B2}$$

where $E_B = \sqrt{M_B^2 + |\mathbf{q}|^2}$ and ω are the energies of the baryon B and the photon, respectively.

For $Q^2 = 0$, one has

$$\omega = |\mathbf{q}| = \frac{M_{B'}^2 - M_B^2}{2M_{B'}}. \tag{B3}$$

Consider now the integral,

$$\mathcal{I}(0) = \int_k \psi_{B'}(P_+, k)\psi_B(P_-, k). \tag{B4}$$

As explained in Sec. III A, the radial wave functions are represented in terms of the variables $\chi_{B'}$ and χ_B, defined by Eq. (2.8). We can rewrite χ_{B^*} in terms of a new variable η_{B^*} defined by

$$\eta_{B^*} \equiv \frac{P_{B^*} \cdot k}{M_{B^*} m_D}, \tag{B5}$$

where B^* holds for B or B'. Then we can write

$$\chi_{B^*} = 2(\eta_{B^*} - 1). \tag{B6}$$

Redefining the diquark momentum $\mathbf{k}$ as $\boldsymbol{\kappa} \equiv \frac{\mathbf{k}}{m_D}$, and the diquark energy as $E_\kappa \equiv \frac{E_D}{m_D}$, we can write

$$\eta_{B'} = E_\kappa = \eta_0, \tag{B7}$$

TABLE IX. One pion-loop contributions to the decuplet baryon self-energies with $\alpha = 0.6$.

B	$g^2 G_{1B}$	$g^2 G_{2B}$
Δ	$g_{\pi N\Delta}^2 \sum_\lambda (\xi_{\pi\lambda} \cdot T^\dagger)(\xi_{\pi\lambda}^* \cdot T) = \frac{8}{25} g^2$	$g_{\pi\Delta\Delta}^2 \sum_\lambda (\xi_{\pi\lambda} \cdot \tau)(\xi_{\pi\lambda}^* \cdot \tau) = g^2$
Σ^*	$g_{\pi\Sigma\Sigma^*}^2 \sum_\lambda (\xi_{\pi\lambda} \cdot \mathbf{J})(\xi_{\pi\lambda}^* \cdot \mathbf{J}) + g_{\pi\Lambda\Sigma^*}^2 \sum_\lambda (\xi_{\pi\lambda} \cdot \xi_{\Sigma^*\mu})(\xi_{\pi\lambda}^* \cdot \xi_{\Sigma^*\mu}^*) = \frac{4}{15} g^2$	$g_{\pi\Sigma^*\Sigma^*}^2 \sum_\lambda (\xi_{\pi\lambda} \cdot \mathbf{J})(\xi_{\pi\lambda}^* \cdot \mathbf{J}) = \frac{8}{15} g^2$
Ξ^*	$g_{\Xi\Xi^*}^2 \sum_\lambda (\xi_{\pi\lambda} \cdot T^\dagger)(\xi_{\pi\lambda}^* \cdot T) = \frac{4}{25} g^2$	$g_{\Xi^*\Xi^*}^2 \sum_\lambda (\xi_{\pi\lambda} \cdot \tau)(\xi_{\pi\lambda}^* \cdot \tau) = \frac{1}{5} g^2$

$$\eta_B = \tilde{E}_B E_\kappa + q_B \kappa_z, \tag{B8}$$

where $\tilde{E}_B = \frac{E_B}{M_B}$, $q_B = \frac{|\mathbf{q}|}{M_B}$ and $\eta_0 \equiv E_\kappa$.

With the above notations, we can write (B4) as

$$\mathcal{I}(0) = \int_{\boldsymbol{\kappa}} \psi_{B'}(\eta_{B'}) \psi_B(\eta_B). \tag{B9}$$

The normalization conditions in the same notations are

$$\int_{\boldsymbol{\kappa}} [\psi_B(\eta_0)]^2 = 1, \tag{B10}$$

$$\int_{\boldsymbol{\kappa}} [\psi_{B'}(\eta_0)]^2 = 1. \tag{B11}$$

Note that, the both conditions are represented in terms of the same argument η_0, since in the rest frame of each particle, all particles have the same value for η_{B^*}.

As shown in Appendix B 2, we can prove that

$$\begin{aligned} \mathcal{I}(0) &= \int_{\boldsymbol{\kappa}} \psi_{B'}(\eta_0) \psi_B(\eta_B), \\ &\leq \int_{\boldsymbol{\kappa}} \psi_{B'}(\eta_0) \psi_B(\eta_0), \end{aligned} \tag{B12}$$

where the equality holds only for the case $M_{B'} = M_B$. Then, using the Cauchy-Schwarz-Hölder inequality for non-negative functions,

$$\left[\int_{\boldsymbol{\kappa}} \psi_{B'}(\eta_0) \psi_B(\eta_0)\right]^2 \leq \left[\int_{\boldsymbol{\kappa}} [\psi_{B'}(\eta_0)]^2\right]\left[\int_{\boldsymbol{\kappa}} [\psi_B(\eta_0)]^2\right], \tag{B13}$$

we conclude from Eqs. (B10) and (B11) that

$$\left|\int_{\boldsymbol{\kappa}} \psi_{B'}(\eta_0) \psi_B(\eta_0)\right| \leq 1. \tag{B14}$$

Combining the result (B14) with (B12) for the case where both radial wave functions are positive, one has

$$\mathcal{I}(0) \leq 1, \tag{B15}$$

where the equality holds only for the case $M_{B'} = M_B$ [when $\eta_{B'} \equiv \eta_B = \eta_0$].

The details of the demonstration of Eq. (B12) are in the next section.

2. Part 2

Here we demonstrate the result given by Eq. (B12).

Consider the integral

$$\mathcal{I}(0) = \int_{\boldsymbol{\kappa}} \psi_{B'}(\eta_0) \psi_B(\eta_B), \tag{B16}$$

where

$$\eta_B = \tilde{E}_B E_\kappa + q_B \kappa_z. \tag{B17}$$

Note that, in the case $M_{B'} = M_B$ one has $q_B = 0$, thus $\eta_B = \eta_0$, and

$$\mathcal{I}(0) = \int_{\boldsymbol{\kappa}} \psi_{B'}(\eta_0) \psi_B(\eta_0). \tag{B18}$$

Consider now the case $q_B > 0$ (when $M_{B'} > M_B$). In this case, according to Eq. (B8), η_B has an angular dependence. Changing the integration variables to $\kappa = \frac{|\mathbf{k}|}{m_D}$ and $z = \cos\theta$, where θ is the angle with $\mathbf{q}$ (z direction), using $\kappa_z = \kappa z$, one can represent Eq. (B16) as

$$\mathcal{I}(0) = m_D^2 \int_0^{+\infty} \frac{\kappa^2 d\kappa}{(2\pi)^2 2E_\kappa} \psi_{B'}(\eta_0) \left[\int_{-1}^{1} dz \psi_B(\eta_B)\right]. \tag{B19}$$

Taking in consideration the definition of ψ_B given by Eqs. (2.9), (2.10), (2.11), and (2.12), we can write ψ_B as

$$\psi_B(\eta_B) = \frac{N_B}{4m_D} \frac{1}{\alpha_i + \eta_B} \frac{1}{\alpha_j + \eta_B}, \tag{B20}$$

where $i, j = 1, 2, 3, 4$, but $i \neq j$, represent the possible indices, and $\alpha_i = \frac{1}{2}(\beta_i - 2)$ with $\alpha_i > -1$ (because $\beta_i > 0$). Using the form (B20), we can now write

$$\mathcal{I}(0) = \frac{m_D N_B}{4} \int_0^{+\infty} \frac{\kappa^2 d\kappa}{(2\pi)^2 2E_\kappa} \psi_{B'}(\eta_0) I_z(q_B), \tag{B21}$$

where

$$I_z(q_B) = \int_{-1}^{1} dz \frac{1}{\alpha_i + \eta_B} \frac{1}{\alpha_j + \eta_B}. \tag{B22}$$

The last function includes all the q_B dependence of the integral $\mathcal{I}(0)$. The κ dependence on $I_z(q_B)$ is omitted for simplicity.

For the present case we can assume that $\alpha_j > \alpha_i$ without loss of generality. Then, the integration in z in (B22) can be performed with the decomposition,

$$I_z(q_B) = \frac{1}{\alpha_j - \alpha_i}\left[\int_{-1}^{1} dz \frac{1}{\alpha_i + \eta_B} - \int_{-1}^{1} dz \frac{1}{\alpha_j + \eta_B}\right]. \tag{B23}$$

Defining

$$\begin{aligned} G(\alpha_i, q_B) &\equiv \int_{-1}^{1} dz \frac{1}{\alpha_i + \eta_B}, \\ &= \frac{1}{q_B \kappa} \log \frac{\alpha_i + \tilde{E}_B E_\kappa + q_B \kappa}{\alpha_i + \tilde{E}_B E_\kappa - q_B \kappa}, \end{aligned} \tag{B24}$$

we can write

$$I_z(q_B) = \frac{1}{\alpha_j - \alpha_i}[G(\alpha_i, q_B) - G(\alpha_j, q_B)]. \tag{B25}$$

The next step is to prove that $I_z(q_B)$ decreases when q_B increases. Performing the derivation in q_B, one has

$$\frac{dI_z}{dq_B} = \frac{1}{\alpha_j - \alpha_i}\left\{-\frac{1}{q_B}[G(\alpha_i, q_B) - G(\alpha_j, q_B)] + [H(\alpha_i, q_B) - H(\alpha_j, q_B)]\right\}, \tag{B26}$$

where

$$H(\alpha_i, q_B) = \frac{1}{q_B\kappa}\left[\frac{1}{\alpha_i + \tilde{E}_B E_\kappa + q_B\kappa} - \frac{1}{\alpha_i + \tilde{E}_B E_\kappa - q_B\kappa}\right]. \tag{B27}$$

Let us consider first the term

$$T_1 = G(\alpha_i, q_B) - G(\alpha_j, q_B). \tag{B28}$$

Using the explicit form given by Eq. (B24), we can write

$$T_1 = \frac{1}{q_B\kappa}\log\frac{\alpha_i\alpha_j + t + (\alpha_i + \alpha_j)\tilde{E}_B E_\kappa + (\alpha_j - \alpha_i)q_B\kappa}{\alpha_i\alpha_j + t + (\alpha_i + \alpha_j)\tilde{E}_B E_\kappa - (\alpha_j - \alpha_i)q_B\kappa}, \tag{B29}$$

where $t = 1 + \kappa^2 + q_B^2$. When $\alpha_j > \alpha_i$, the argument of the log function, u, is larger than 1. Therefore $\log u > 0$ and

$$T_1 > 0, \tag{B30}$$

when $\alpha_j > \alpha_i$.

Consider now

$$T_2 = H(\alpha_i, q_L) - H(\alpha_j, q_L). \tag{B31}$$

Working with the expression (B27), we obtain,

$$H(\alpha_i, q_L) = -\frac{1}{(\alpha_i + \tilde{E}_B E_\kappa)^2 - q_B^2\kappa^2}. \tag{B32}$$

Therefore,

$$T_2 = \frac{1}{(\alpha_j + \tilde{E}_B E_\kappa)^2 - q_B^2\kappa^2} - \frac{1}{(\alpha_i + \tilde{E}_B E_\kappa)^2 - q_B^2\kappa^2}. \tag{B33}$$

If $\alpha_j > \alpha_i$, one has

$$T_2 < 0. \tag{B34}$$

Combining the results (B30) and (B34), we conclude that

$$\frac{dI_z}{dq_B}(q_B) < 0, \tag{B35}$$

when $\alpha_j > \alpha_i$. As a consequence $I_z(q_B)$ decreases with increasing q_B for $q_B > 0$, and

$$I_z(q_B) \leq I_z(0), \tag{B36}$$

where the equality holds only when $q_B = 0$.

As $I_z(q_B)$ includes only the q_B dependence in $\mathcal{I}(0)$, we conclude also that $\mathcal{I}(0)$ is a decreasing function of q_B. Furthermore, since $\mathcal{I}(0)$ is a continuous function of q_B, the maximum value for $\mathcal{I}(0)$ is obtained for the minimum value of q_B, the case $q_B = 0$, when $\eta_B = \eta_0$. Therefore,

$$\mathcal{I}(0) < \int_\kappa \psi_{B'}(\eta_0)\psi_B(\eta_0), \tag{B37}$$

if $q_B > 0$, and

$$\mathcal{I}(0) = \int_\kappa \psi_{B'}(\eta_0)\psi_B(\eta_0), \tag{B38}$$

if $q_B = 0$.

APPENDIX C: PION CLOUD DRESSING

In this Appendix we present the expressions for the pion cloud contributions. We assume that the leading contribution for the pion cloud dressing is given by the diagram with a direct coupling of a photon to pion. We assume also that in the first approximation, the pion baryon vertex can be represented by the results of the cloudy bag model (CBM) [74–76], with the couplings determined by $SU(6)$ symmetry. A similar approximation was also used in Ref. [49].

In this description the pion cloud contributions for the magnetic transition form factors are determined by a function $F_{BB'}$, where B (B') stands for the initial (final) state baryon.

Note that the function $F_{BB'}$ can be a sum of different amplitudes associated with the several intermediate baryon

TABLE X. Pion cloud contributions for G_M^*, expressed in terms of the function $F_{BB'}$ (combination of the integrals $H_{BB'}(B_1)$).

	$F_{BB'}$
$\gamma^* N \to \Delta$	$F_{N\Delta} = \frac{4}{15\sqrt{3}}[H_{N\Delta}(N) + 5H_{N\Delta}(\Delta)]$
$\gamma^* \Lambda \to \Sigma^*$	$F_{\Lambda\Sigma^*} = \frac{8}{75}[H_{\Lambda\Sigma^*}(\Sigma) + 5H_{\Lambda\Sigma^*}(\Sigma^*)]$
$\gamma^* \Sigma \to \Sigma^*$	$F_{\Sigma\Sigma^*} = \frac{4}{75\sqrt{3}}[3H_{\Sigma\Sigma^*}(\Lambda) - 2H_{\Sigma\Sigma^*}(\Sigma) + 5H_{\Sigma\Sigma^*}(\Sigma^*)]J_3$
$\gamma^* \Xi \to \Xi^*$	$F_{\Xi\Xi^*} = \frac{4}{75\sqrt{3}}[H_{\Xi\Xi^*}(\Xi) + 5H_{\Xi\Xi^*}(\Xi^*)]\tau_3$

TABLE XI. Function $F_{BB'}$ in the $SU(3)$ limit $H_{BB'}(B_1) = H$. The last column gives the result in terms of that for $F_{N\Delta}$.

	$F_{BB'}(H)$	$F_{BB'}(F_{N\Delta})$
$\gamma^* N \to \Delta$	$\frac{8}{5\sqrt{3}} H$	$F_{N\Delta}$
$\gamma^* \Lambda \to \Sigma^*$	$\frac{16}{25} H$	$\frac{2\sqrt{3}}{5} F_{N\Delta}$
$\gamma^* \Sigma \to \Sigma^*$	$\frac{8}{25\sqrt{3}} H J_3$	$\frac{1}{5} F_{N\Delta} J_3$
$\gamma^* \Xi \to \Xi^*$	$\frac{8}{25\sqrt{3}} H \tau_3$	$\frac{1}{5} F_{N\Delta} \tau_3$

B_1 states (octet or decuplet baryons) as shown in Fig. 1. Taking into account the possible spin and flavor states, we can reduce the function $F_{BB'}(B_1)$ to a combination of scalar integral $H_{BB'}(B_1)$.

The results of the pion cloud contributions are presented in Table X. We note that the analysis can be extended to the kaon and η-meson clouds; however, these meson contributions are known to be smaller than those of the pion [76], and thus we consider only the processes with the pion loops in this study.

Finally, under an $SU(3)$ symmetry, where all the octet members have a unique mass M_B and all the decuplet members have a unique mass $M_{B'}$, we can replace $H_{BB'}(B_1)$ by one single function H for all the cases of the $\gamma^* B \to B'$ reactions. The results for this symmetry limit are presented in Table XI. In this case, all the functions $F_{BB'}$ can be expressed in terms of the result for the $\gamma^* N \to \Delta$ case ($F_{N\Delta}$), as shown in the last column of Table XI.

[1] V. Pascalutsa, M. Vanderhaeghen, and S. N. Yang, Phys. Rep. **437**, 125 (2007).
[2] V. D. Burkert and T. S. H. Lee, Int. J. Mod. Phys. E **13**, 1035 (2004).
[3] I. G. Aznauryan, A. Bashir, V. Braun, S. J. Brodsky, V. D. Burkert, L. Chang, C. Chen, and B. El-Bennich *et al.*, Int. J. Mod. Phys. E **22**, 1330015 (2013).
[4] K. Nakamura *et al.* (Particle Data Group), J. Phys. G **37**, 075021 (2010).
[5] D. Keller *et al.* (CLAS Collaboration), Phys. Rev. D **83**, 072004 (2011).
[6] D. Keller *et al.* (CLAS Collaboration), Phys. Rev. D **85**, 059903 (2012).
[7] S. Taylor *et al.* (CLAS Collaboration), Phys. Rev. C **71**, 054609 (2005); **72**, 039902(E) (2005).
[8] V. V. Molchanov *et al.* (SELEX Collaboration), Phys. Lett. B **590**, 161 (2004).
[9] H. J. Lipkin, Phys. Rev. D **7**, 846 (1973).
[10] R. Koniuk and N. Isgur, Phys. Rev. D **21**, 1868 (1980); **23**, 818(E) (1981).
[11] J. W. Darewych, M. Horbatsch, and R. Koniuk, Phys. Rev. D **28**, 1125 (1983).
[12] E. Kaxiras, E. J. Moniz, and M. Soyeur, Phys. Rev. D **32**, 695 (1985).
[13] M. Warns, H. Schroder, W. Pfeil, and H. Rollnik, Z. Phys. C **45**, 613 (1990); M. Warns, W. Pfeil, and H. Rollnik, Phys. Lett. B **258**, 431 (1991).
[14] R. K. Sahoo, A. R. Panda, and A. Nath, Phys. Rev. D **52**, 4099 (1995).
[15] G. Wagner, A. J. Buchmann, and A. Faessler, Phys. Rev. C **58**, 1745 (1998).
[16] L. Tiator, D. Drechsel, S. Kamalov, M. M. Giannini, E. Santopinto, and A. Vassallo, Eur. Phys. J. A **19**, 55 (2004).
[17] N. Sharma, H. Dahiya, P. K. Chatley, and M. Gupta, Phys. Rev. D **81**, 073001 (2010).
[18] N. Sharma and H. Dahiya, Pramana **80**, 237 (2013).
[19] E. Santopinto and M. M. Giannini, Phys. Rev. C **86**, 065202 (2012).
[20] C. L. Schat, C. Gobbi, and N. N. Scoccola, Phys. Lett. B **356**, 1 (1995).
[21] A. Abada, H. Weigel, and H. Reinhardt, Phys. Lett. B **366**, 26 (1996).
[22] T. Haberichter, H. Reinhardt, N. N. Scoccola, and H. Weigel, Nucl. Phys. A **615**, 291 (1997).
[23] L. Wang and F. X. Lee, Phys. Rev. D **80**, 034003 (2009).
[24] M. N. Butler, M. J. Savage, and R. P. Springer, Nucl. Phys. B **399**, 69 (1993).
[25] M. N. Butler, M. J. Savage, and R. P. Springer, Phys. Lett. B **304**, 353 (1993).
[26] D. Arndt and B. C. Tiburzi, Phys. Rev. D **69**, 014501 (2004).
[27] R. F. Lebed and R. H. TerBeek, Phys. Rev. D **83**, 016009 (2011).
[28] R. Bijker, F. Iachello, and A. Leviatan, Ann. Phys. (N.Y.) **284**, 89 (2000).
[29] D. B. Leinweber, T. Draper, and R. M. Woloshyn, Phys. Rev. D **48**, 2230 (1993).
[30] C. Alexandrou, Ph. de Forcrand, H. Neff, J. W. Negele, W. Schroers, and A. Tsapalis, Phys. Rev. Lett. **94**, 021601 (2005); C. Alexandrou, Ph. de Forcrand, Th. Lippert, H. Neff, J. W. Negele, K. Schilling, W. Schroers, and A. Tsapalis, Phys. Rev. D **69**, 114506 (2004).
[31] C. Alexandrou, G. Koutsou, H. Neff, J. W. Negele, W. Schroers, and A. Tsapalis, Phys. Rev. D **77**, 085012 (2008).
[32] G. Ramalho, M. T. Peña and F. Gross, Eur. Phys. J. A **36**, 329 (2008).
[33] G. Ramalho, M. T. Peña and F. Gross, Phys. Rev. D **78**, 114017 (2008).
[34] G. Ramalho, K. Tsushima, and A. W. Thomas, J. Phys. G **40**, 015102 (2013).
[35] G. Ramalho and K. Tsushima, Phys. Rev. D **84**, 054014 (2011).
[36] F. Gross, G. Ramalho, and K. Tsushima, Phys. Lett. B **690**, 183 (2010).

[37] G. Ramalho, K. Tsushima, and F. Gross, Phys. Rev. D **80**, 033004 (2009).

[38] G. Ramalho, F. Gross, M. T. Peña and K. Tsushima, in *Proceedings of the 4th Workshop on Exclusive Reactions at High Momentum Transfer*, edited by A. Radyushkin (World Scientific, Singapore, 2011), p. 287.

[39] F. Gross, G. Ramalho, and M. T. Peña, Phys. Rev. C **77**, 015202 (2008).

[40] F. Gross, G. Ramalho, and M. T. Peña, Phys. Rev. D **85**, 093005 (2012); **85**, 093006 (2012).

[41] F. Gross, G. Ramalho, and M. T. Peña, Phys. Rev. C **77**, 035203 (2008).

[42] G. Ramalho, M. T. Peña and F. Gross, Phys. Lett. B **678**, 355 (2009).

[43] G. Ramalho, M. T. Peña and F. Gross, Phys. Rev. D **81**, 113011 (2010).

[44] G. Ramalho, M. T. Peña and A. Stadler, Phys. Rev. D **86**, 093022 (2012).

[45] G. Ramalho and M. T. Peña, Phys. Rev. D **83**, 054011 (2011).

[46] G. Ramalho and M. T. Peña, Phys. Rev. D **80**, 013008 (2009).

[47] G. Ramalho and M. T. Peña, J. Phys. G **36**, 115011 (2009).

[48] G. Ramalho and K. Tsushima, Phys. Rev. D **81**, 074020 (2010); G. Ramalho and M. T. Peña, Phys. Rev. D **84**, 033007 (2011).

[49] G. Ramalho and K. Tsushima, Phys. Rev. D **82**, 073007 (2010).

[50] G. Ramalho and K. Tsushima, Phys. Rev. D **86**, 114030 (2012); G. Ramalho, D. Jido, and K. Tsushima, Phys. Rev. D **85**, 093014 (2012).

[51] F. Gross, Phys. Rev. **186**, 1448 (1969); A. Stadler, F. Gross, and M. Frank, Phys. Rev. C **56**, 2396 (1997).

[52] S. Boinepalli, D. B. Leinweber, P. J. Moran, A. G. Williams, J. M. Zanotti, and J. B. Zhang, Phys. Rev. D **80**, 054505 (2009).

[53] M. D. Sanctis, M. M. Giannini, E. Santopinto, and A. Vassallo, Phys. Rev. C **76**, 062201 (2007).

[54] C. Amsler *et al.* (Particle Data Group), Phys. Lett. B **667**, 1 (2008). See p. 1023 for information about the naive quark model.

[55] L. Chang, Y.-X. Liu and C. D. Roberts, Phys. Rev. Lett. **106**, 072001 (2011).

[56] D. J. Wilson, I. C. Cloet, L. Chang, and C. D. Roberts, Phys. Rev. C **85**, 025205 (2012).

[57] F. Cardarelli, E. Pace, G. Salme, and S. Simula, Phys. Lett. B **357**, 267 (1995).

[58] H. Ito, Phys. Rev. C **52**, R1750 (1995).

[59] J. J. Kelly, Phys. Rev. C **56**, 2672 (1997).

[60] Z. Batiz and F. Gross, Phys. Rev. C **58**, 2963 (1998).

[61] H. F. Jones and M. D. Scadron, Ann. Phys. (N.Y.) **81**, 1 (1973).

[62] W. Bartel, B. Dudelzak, H. Krehbiel, J. McElroy, U. Meyer-Berkhout, W. Schmidt, V. Walther, and G. Weber, Phys. Lett. B **28**, 148 (1968).

[63] S. Stein, W. Atwood, E. Bloom, R. Cottrell, H. DeStaebler, C. Jordan, H. Piel, C. Prescott, R. Siemann, and R. Taylor, Phys. Rev. D **12**, 1884 (1975).

[64] K. Joo *et al.* (CLAS Collaboration), Phys. Rev. Lett. **88**, 122001 (2002); I. G. Aznauryan *et al.* (CLAS Collaboration), Phys. Rev. C **80**, 055203 (2009).

[65] L. Tiator, D. Drechsel, O. Hanstein, S. S. Kamalov, and S. N. Yang, Nucl. Phys. A **689**, 205 (2001).

[66] D. Drechsel, S. S. Kamalov, and L. Tiator, Eur. Phys. J. A **34**, 69 (2007).

[67] T. Sato and T. S. H. Lee, Phys. Rev. C **63**, 055201 (2001).

[68] B. Julia-Diaz, T. S. H. Lee, T. Sato, and L. C. Smith, Phys. Rev. C **75**, 015205 (2007).

[69] S. S. Kamalov, S. N. Yang, D. Drechsel, O. Hanstein, and L. Tiator, Phys. Rev. C **64**, 032201 (2001).

[70] C. E. Carlson, Phys. Rev. D **34**, 2704 (1986); C. E. Carlson, in $e+e-$ *Physics at Intermediate-Energies, Stanford, USA, 2001*, edited by D. Bettoni, eConf C010430, W09 (2001).

[71] G. Wolf, G. Batko, W. Cassing, U. Mosel, K. Niita, and M. Schaefer, Nucl. Phys. A **517**, 615 (1990).

[72] G. Ramalho and M. T. Peña, Phys. Rev. D **85**, 113014 (2012).

[73] S. Capstick and B. D. Keister, Phys. Rev. D **51**, 3598 (1995).

[74] A. W. Thomas, Adv. Nucl. Phys. **13**, 1 (1984).

[75] S. Theberge and A. W. Thomas, Nucl. Phys. A **393**, 252 (1983).

[76] K. Tsushima, T. Yamaguchi, M. Takizawa, Y. Kohyama, and K. Kubodera, Phys. Lett. B **205**, 128 (1988); K. Tsushima, T. Yamaguchi, Y. Kohyama, and K. Kubodera, Nucl. Phys. A **489**, 557 (1988); T. Yamaguchi, K. Tsushima, Y. Kohyama, and K. Kubodera, Nucl. Phys. A **500**, 429 (1989).

[77] V. V. Frolov *et al.*, Phys. Rev. Lett. **82**, 45 (1999); M. Ungaro *et al.* (CLAS Collaboration), Phys. Rev. Lett. **97**, 112003 (2006); A. N. Villano, P. Stoler, P. E. Bosted, S. H. Connell, M. M. Dalton, M. K. Jones, V. Kubarovsky, and G. S. Adams *et al.*, Phys. Rev. C **80**, 035203 (2009).